

## Carbonates in the Critical Zone

M. D. Covington<sup>1,2</sup>, J. B. Martin<sup>3</sup>, L. E. Toran<sup>4</sup>, J. L. Macalady<sup>5</sup>, P. L. Sullivan<sup>6</sup>, Á. A. García, Jr.<sup>7</sup>, J. B. Heffernan<sup>8</sup>, and W. D. Graham<sup>9</sup>

<sup>1</sup>Department of Geosciences, University of Arkansas, Fayetteville, AR, USA. <sup>2</sup>ZRC SAZU, Karst Research Institute, Slovenia. <sup>3</sup>Department of Geological Sciences, University of Florida, Gainesville, FL, USA. <sup>4</sup>Department of Earth and Environmental Science, Temple University, Philadelphia, PA, USA <sup>5</sup>Department of Geosciences, Pennsylvania State University, State College, PA, USA <sup>6</sup>College of Earth, Ocean, and Atmospheric Science, Oregon State University, OR, USA <sup>7</sup>Department of Geology and Environmental Science, James Madison University, Harrisonburg, VA, USA <sup>8</sup>Nicholas School of the Environment, Duke University, Durham, NC <sup>9</sup>University of Florida Water Institute, Gainesville, FL, USA

Corresponding author: Matthew D. Covington ([mcoving@uark.edu](mailto:mcoving@uark.edu))

### Key Points:

- A holistic understanding of Earth's critical zone requires integrative studies spanning the spectrum of carbonate and silicate landscapes.
- Porosity developed by congruent dissolution of carbonates decouples hillslopes from stream channels, altering topographic equilibrium.
- Shifts in carbonate critical zone structure from changing ecology, land use, and climate may be rapid because of fast dissolution kinetics.

## 20 **Abstract**

21 Earth's Critical Zone (CZ), the near-surface layer where rock is weathered and landscapes co-  
22 evolve with life, is profoundly influenced by the type of underlying bedrock. Previous studies of  
23 the CZ have focused almost exclusively on landscapes dominated by silicate rocks. However,  
24 carbonate rocks crop out on approximately 15% of Earth's ice-free continental surface and  
25 provide important water resources and ecosystem services to ~1.2 billion people. Unlike  
26 silicates, carbonate minerals weather congruently and have high solubilities and rapid dissolution  
27 kinetics, enabling the development of large, interconnected pore spaces and preferential flow  
28 paths that restructure the CZ. Here we review the state of knowledge of the carbonate CZ and  
29 examine whether current conceptual models of the CZ, such as the conveyor model, can be  
30 applied to carbonate landscapes. We introduce the concept of a carbonate-silicate CZ spectrum.  
31 To obtain a holistic understanding of Earth's CZ we must understand CZ processes and  
32 architecture along the entire spectrum between the carbonate and silicate endmembers. We  
33 explore parameters that produce contrasts in the CZ in different carbonate settings and identify  
34 important open questions about carbonate CZ processes. We argue that, to advance beyond site-  
35 specific understanding and develop a more general conceptual framework for the role of  
36 carbonates in the CZ, we need integrative studies spanning both the carbonate-silicate spectrum  
37 and a range of carbonate settings.

## 38 **Plain Language Summary**

39 Most studies of the critical zone, which is the locus of mineral weathering and life processes,  
40 focus on landscapes underlain by silicate minerals. However, in landscapes underlain by  
41 carbonate minerals the critical zone has different weathering characteristics than in landscapes  
42 underlain predominately by silicate minerals. Consequently, carbonate landscapes, which cover  
43 ~15% of Earth's land surface and provide critical water resources and other services to ~1.2  
44 billion people, require similar focused studies. This review of the state of knowledge of the  
45 carbonate critical zone places it in the spectrum of carbonate to silicate dominated landscapes  
46 and reveals that a standard model of silicate critical zone evolution, the conveyor model, requires  
47 modifications to include loss of dissolved and solid weathering products through pathways  
48 unique to carbonate systems. The review also describes contrasts in the critical zone across  
49 carbonate landscapes and within the range of rock types between pure carbonate and pure  
50 silicates, examining factors such as the depth of the base of the critical zone, water and energy  
51 flow through the critical zone, and variations in surface vegetation. Integrative studies of silicate,  
52 carbonate, and mixed silicate-carbonate landscapes will be required to further a holistic  
53 understanding of Earth's critical zone.

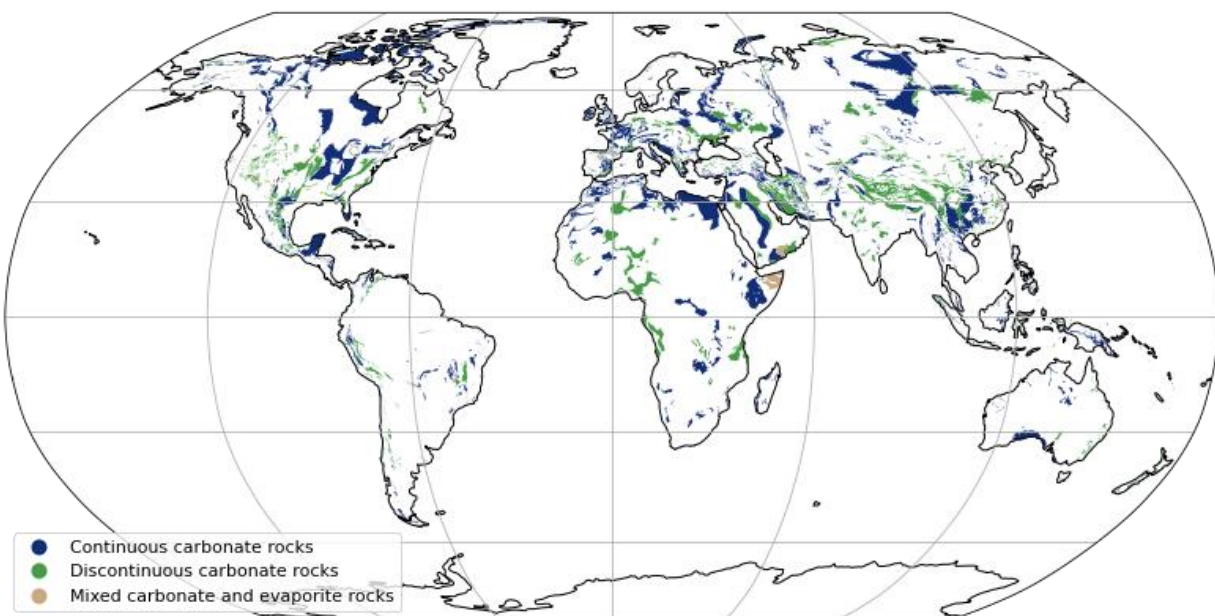
54

## 55 **1 Introduction**

56 The objectives of this paper are to review the state of knowledge of critical zone (CZ)  
57 processes in carbonate terrains, to advance a framework that serves to bridge the spectrum  
58 between carbonate and silicate CZ endmembers (Martin et al., 2021), and to identify key  
59 knowledge gaps in our understanding of the carbonate CZ. Earth's CZ is the region where  
60 landscapes co-evolve with life and is loosely defined as the zone from the base of continental  
61 crust weathering to the top of vegetation canopy (National Research Council, 2001). The CZ  
62 develops through interactions among geological, hydrological, chemical, biological, and climate  
63 processes. Understanding the scope of, and linkages between, these interactions requires

64 interdisciplinary collaborations, to unravel how the CZ functions and responds to environmental  
65 perturbations, including human impacts on climate, land use, and global elemental cycling. The  
66 U.S. scientific community initially engaged in focused research on Earth's CZ through the  
67 development of place-based Critical Zone Observatories (CZO) (Brantley et al., 2017b) and  
68 more recently has developed theme-based Critical Zone Networks (CZNs). The CZO/CZN sites  
69 span a variety of geological and climate settings across the U.S. However, the CZ framework is  
70 limited by a CZO/CZN focus on landscapes underlain by silicate rocks (Martin et al., 2021).  
71 Although existing studies provide useful information about specific carbonate terrains, more  
72 synthesis and a better predictive understanding of the carbonate CZ will require consideration of  
73 multiple carbonate settings with varied characteristics. Such a synthesis could also improve  
74 fundamental understanding of the silicate dominated CZ, as weathering of carbonates is also  
75 important within (pre-)dominantly silicate settings, and landscapes fall on a continuum between  
76 the carbonate and silicate endmembers.

77 A focus on terrains where the CZ is dominated by carbonate minerals is justified by their  
78 common occurrence, their influence on society and its resource base, and their role in the human  
79 experience and human culture. Approximately 15% of Earth's ice-free continental surface  
80 contains carbonate rock (Figure 1), and approximately 1.2 billion people, 16% of the Earth's  
81 population, reside on carbonate rock (Goldscheider et al., 2020). Landscapes developed by the  
82 dissolution of carbonate terrains, also known as karst, often appear as a central theme in cultural  
83 development among long-term communities around the world. Karst landforms and features  
84 have influenced Indigenous creation stories, place-naming (toponymy), culturally based  
85 geological interpretation, and local language adaptation in the Greater Antilles part of the  
86 Caribbean (Alvarez Nazario 1972; Dominguez-Cristobal 1989, 1992, 2007; Garcia et al., 2020;  
87 Pané 1999), as well as a form of wealth building in central Europe that goes back to the 17th  
88 century (Zorn et al., 2009). In addition, the conservation of karst features is becoming a global  
89 priority because they commonly link geological, ecological, cultural, archeological, and touristic  
90 resources (Williams, 2008a).



91 **Figure 1.** Carbonate exposures across the surface of earth using data from the World Karst  
92 Aquifer Map (data from Goldscheider et al., 2020).  
93

94

95 Carbonate terrains provide a wide range of societal and ecological services and present a  
96 variety of unique hazards. Given the favorable conditions for groundwater extraction from  
97 carbonates, and the ubiquity of springs within carbonate terrains, aquifers that develop in  
98 carbonate rocks are a crucial component of the global water supply (Ford and Williams, 2007;  
99 Worthington et al., 2016). Carbonate terrains also host a variety of unique hazards, such as  
100 sinkholes and groundwater flooding, which cause significant economic losses in densely  
101 populated areas (De Waele et al., 2011). Carbonate aquifers are particularly susceptible to  
102 contamination due to rapid travel times and limited natural remediation within large pores and  
103 conduits (White et al., 2016). Carbonate rocks are the largest global reservoir of carbon and have  
104 a potentially important, yet uncertain, role in the global carbon cycle over timescales relevant for  
105 rapid climate change (Gaillardet et al., 2019; Martin, 2017). Nearly pure carbonate rocks provide  
106 the raw materials for cement manufacturing by calcination converting  $\text{CaCO}_3$  to  $\text{CaO}$  plus  $\text{CO}_2$ ,  
107 thereby producing 13% of the world's industrial  $\text{CO}_2$  emissions (Fischedick et al., 2014).  
108 Carbonate minerals provide important pH buffering capacity within aquatic systems.  
109 Subterranean habitats within carbonate terrains host a wide variety of endemic species, many of  
110 which are threatened or endangered (Culver and Pipan, 2013). Interpretation of speleothem  
111 records within caves, which are an important source of paleoclimate information, requires  
112 substantial understanding of carbonate CZ processes, as signals recorded in speleothems are first  
113 filtered through the upper portion of the CZ (Fairchild et al., 2006; Fohlmeister et al., 2020).  
114 Because of rapid mineral dissolution processes within, and subsurface fluxes through, the  
115 carbonate CZ, it has been suggested that carbonate CZ systems may act as a bellwether for CZ  
116 response to climatic and human perturbations (Sullivan et al., 2017). Furthermore, carbonate  
117 minerals often make up an important component of other sedimentary rocks (Hartmann and  
118 Moosdorf, 2012).

## 119 **2 The carbonate-silicate spectrum**

120 A fundamental difference between the carbonate and silicate CZ endmembers is the  
121 spatial pattern and extent of rock dissolution. Carbonate-dominated landscapes, which  
122 experience rapid and extensive dissolution, are characterized by dolines (also called sinkholes),  
123 springs, caves, and deranged surface drainage networks (Ford and Williams, 2007), while  
124 silicate-dominated landscapes rarely have these characteristics. Due to fundamental differences  
125 in the properties of silicate and carbonate mineral groups, the percentage and spatial distribution  
126 of carbonate minerals within parent rocks drive other important differences in the processes and  
127 architectures that develop as the CZ evolves. As a conceptual framework, we will consider a  
128 silicate-carbonate spectrum (Figure 2), with endmember landscapes completely dominated by  
129 either carbonate or silicate minerals. This framework provides a link between prior CZ studies  
130 and synthesis studies yet to be carried out in both carbonate and silicate-dominated sites along  
131 the spectrum. Understanding how CZ dynamics and processes change along this spectrum is a  
132 crucial next step towards integrating carbonate landscapes into existing knowledge of the CZ.  
133 We argue that formally considering the carbonate CZ will also contribute to new understanding  
134 of silicate settings by comparison.

### 135 **2.1 Silicate-carbonate mineral mixtures and distributions in the CZ**

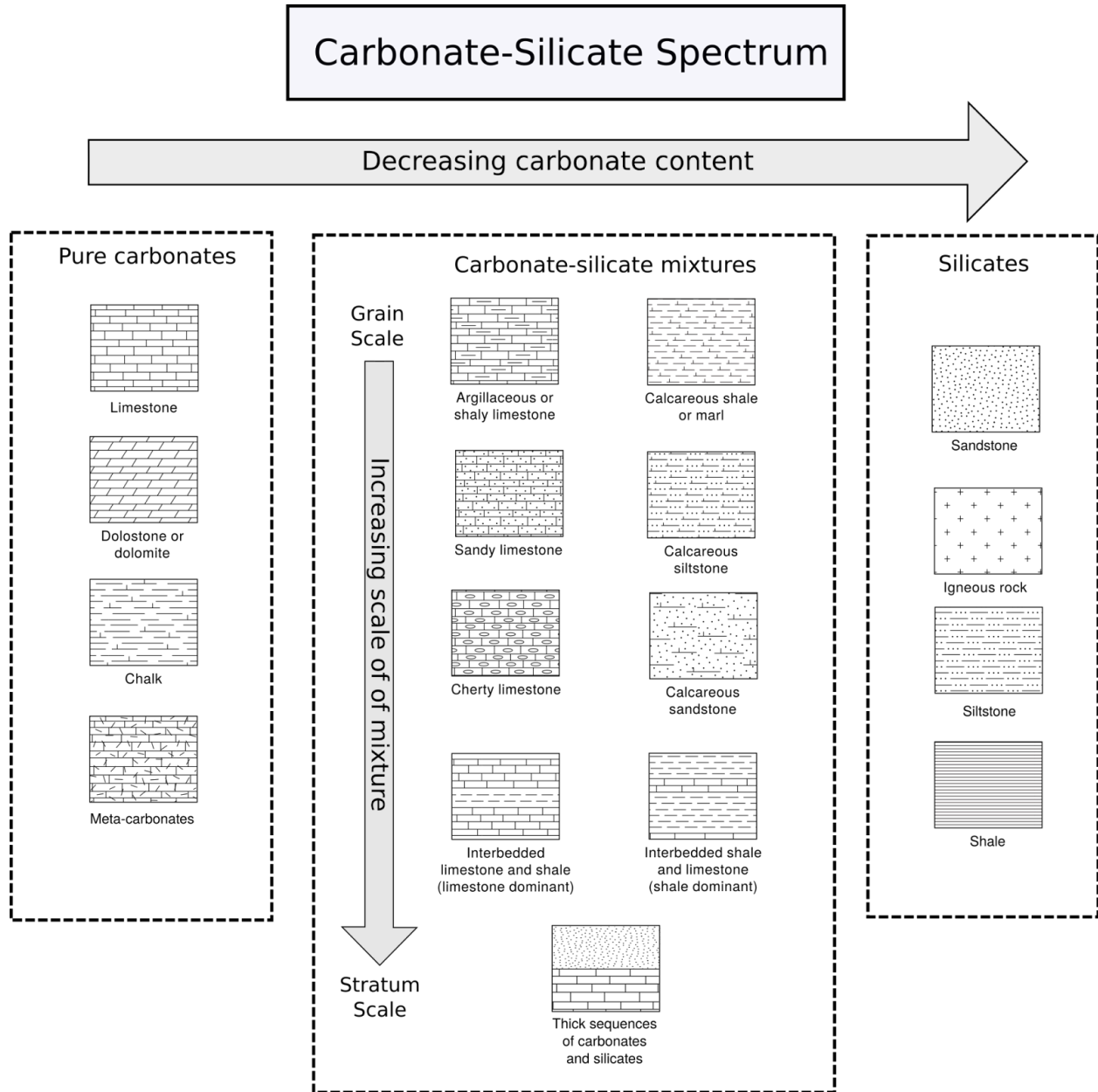
136 Within Earth's CZ, silicate and carbonate minerals mix across a range of scales, from the  
137 grain scale to stratigraphic scales (Figure 2). At the grain scale, all carbonate rocks contain some  
138 percentage of non-carbonate minerals, with common constituents including clays and slowly

139 weathering silicate minerals such as quartz and feldspars (Ford and Williams, 2007). Silicate  
140 mineral fractions of carbonate rocks often take the form of sand- or silt-size quartz grains, or  
141 nodules or beds of authigenic chert (Figure 3a). These minerals may remain as lag deposits as the  
142 carbonate minerals are dissolved (Figure 3b-c). Similarly, many siliciclastic rocks contain some  
143 fraction of carbonate minerals, often in the form of a cement between grains. Calcite-cemented  
144 sandstones, or impure carbonates, can form cave and karst landforms through the process of  
145 phantomization (Dubois et al., 2014; Häuselmann and Tognini, 2005; Kůrková et al., 2019),  
146 whereby preferential dissolution of the cement disintegrates the rock and then the remaining  
147 loose sand grains are removed physically by piping (Figure 3d). Counterintuitively, the  
148 effectiveness of the phantomization process is only weakly dependent on calcite percentage, and  
149 instead disintegration is largely controlled by the grain-size and texture of the silicate component  
150 (Kůrková et al., 2019). This observation suggests that the change of landforms and CZ  
151 architecture along the carbonate-silicate spectrum depends on variables other than just the  
152 carbonate fraction of the lithology, such as how the mineral groups are distributed at the grain  
153 scale.

154 In addition to mixtures at the grain scale, silicate and carbonate rocks occur as relatively  
155 pure beds in layered stratigraphy (Figure 2). Terrains composed largely of carbonates may  
156 contain continuous beds of non-carbonates such as chert or shale. The layering creates  
157 heterogeneities in porosity and permeability with silicate mineral layers often less permeable  
158 than carbonate layers. The contrasts in permeability can create perched water tables and zones of  
159 focused conduit development in the carbonate layers (Figure 3e), while the impermeable silicate  
160 mineral layers tend to impede vertical flow of water. Sometimes carbonates are thinly  
161 interbedded with impure carbonates, shales, or other non-carbonate rocks, creating a landscape  
162 referred to as merokarst (Cvijic, 1925). Merokarst typically displays little surface topographical

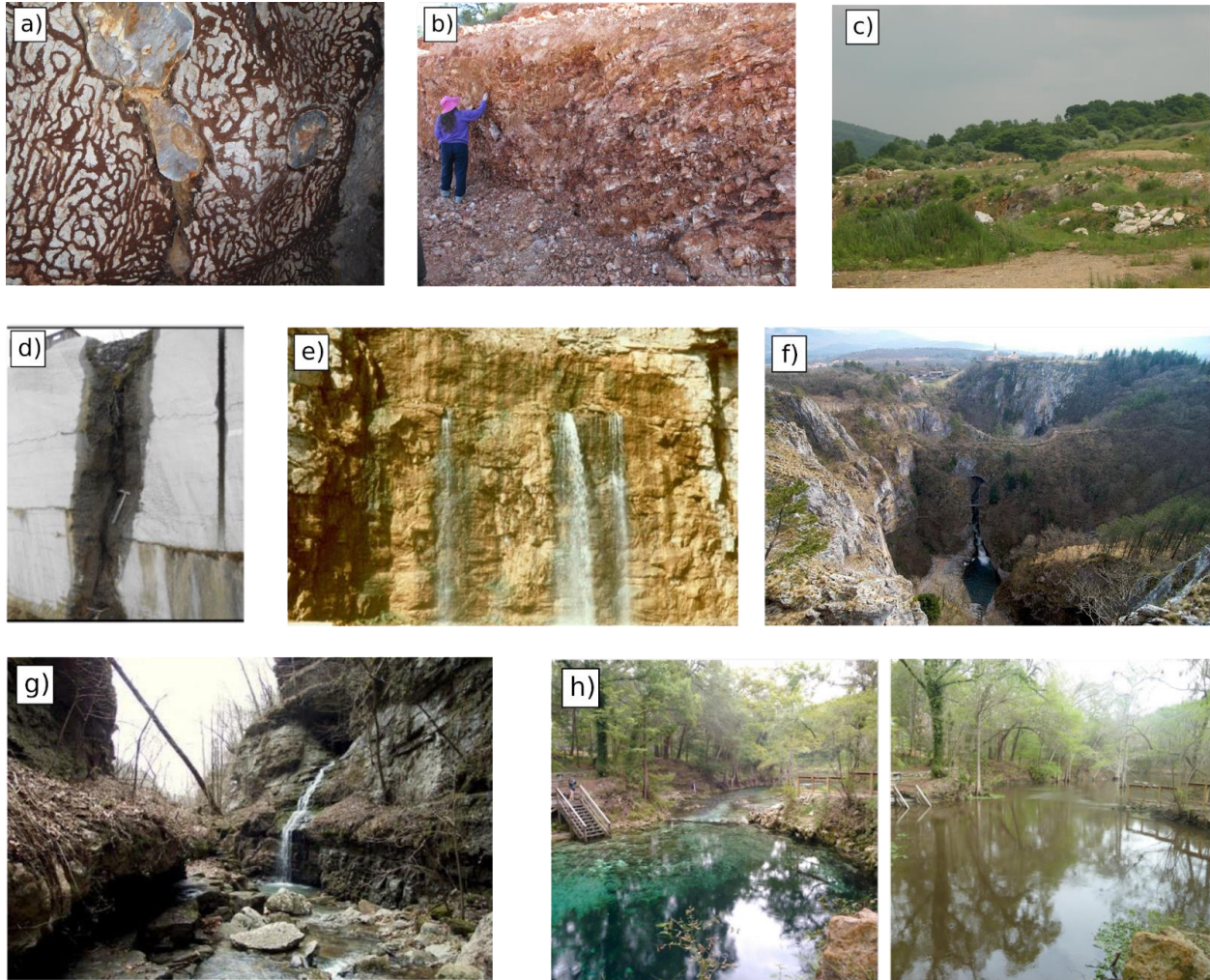
163 expression of karst but may still behave hydrologically like a karst system (Brookfield et al.,  
 164 2017; Macpherson and Sullivan, 2019a; Sullivan et al. 2020).

165



166 **Figure 2.** The carbonate-silicate spectrum. In addition to end-member cases of pure carbonate  
 167 and silicate rocks, carbonates and silicates commonly occur as mixtures. Both the carbonate  
 168 percentage and the scale over which the two mineral types mix are crucial parameters that will  
 169 influence critical zone structure and evolution.  
 170

171  
 172  
 173  
 174  
 175



176  
 177 **Figure 3.** a) Differential weathering of chert nodules within micritic limestone in Grotta Sulfurea,  
 178 Frasassi, Italy. The cave walls are colonized by microbial biofilms (biovermiculations) that prefer  
 179 the carbonate to the silicate surface, b) A thick regolith layer of chert and clay left behind after  
 180 dissolution of the Boone Limestone, Arkansas, c) Weathering residuum drapes crystalline  
 181 dolomite of the Cambrian Ledger Formation in Pennsylvania, d) Ghost-rock karstification  
 182 (phantomization), whereby weathering residuum is left behind within solutionally altered  
 183 preferential flow paths, near Soignies, Belgium (from Dubois et al., 2014), e) Water emerges  
 184 from a bedding plane on top of a chert layer within a carbonate rock, Arkansas, f) The Reka  
 185 River in the classical karst region of Slovenia sinks after flowing from flysch onto limestone,  
 186 creating two large 160-m deep collapse dolines and the upper entrance to Škocjan Caves, g) A  
 187 perched spring creates a waterfall at the contact where a limestone unit overlies a sandstone,  
 188 Indian Creek, Arkansas, h) Madison Blue Spring, Florida, an estavelle, which functions as a  
 189 spring in baseflow conditions (left) and reverses flow direction to receive organic-rich water from  
 190 the Withlacoochee River during flood events (right).

191 Thick carbonate layers may be juxtaposed laterally with non-carbonate rocks. Contacts  
 192 between carbonates and non-carbonates that are exposed at the surface typically form regions of  
 193 intense interaction between surface and subsurface hydrological, geomorphological, and  
 194 biological processes (Atkinson, 1977a; Brucker et al., 1972; Gulley et al., 2013; Khadka et al.,  
 195 2014; Martin and Dean, 1999; Palmer, 2001). When surface water flows from non-carbonate  
 196 onto carbonate rocks, sinking streams, blind valleys, sinkholes, and open cave shafts often

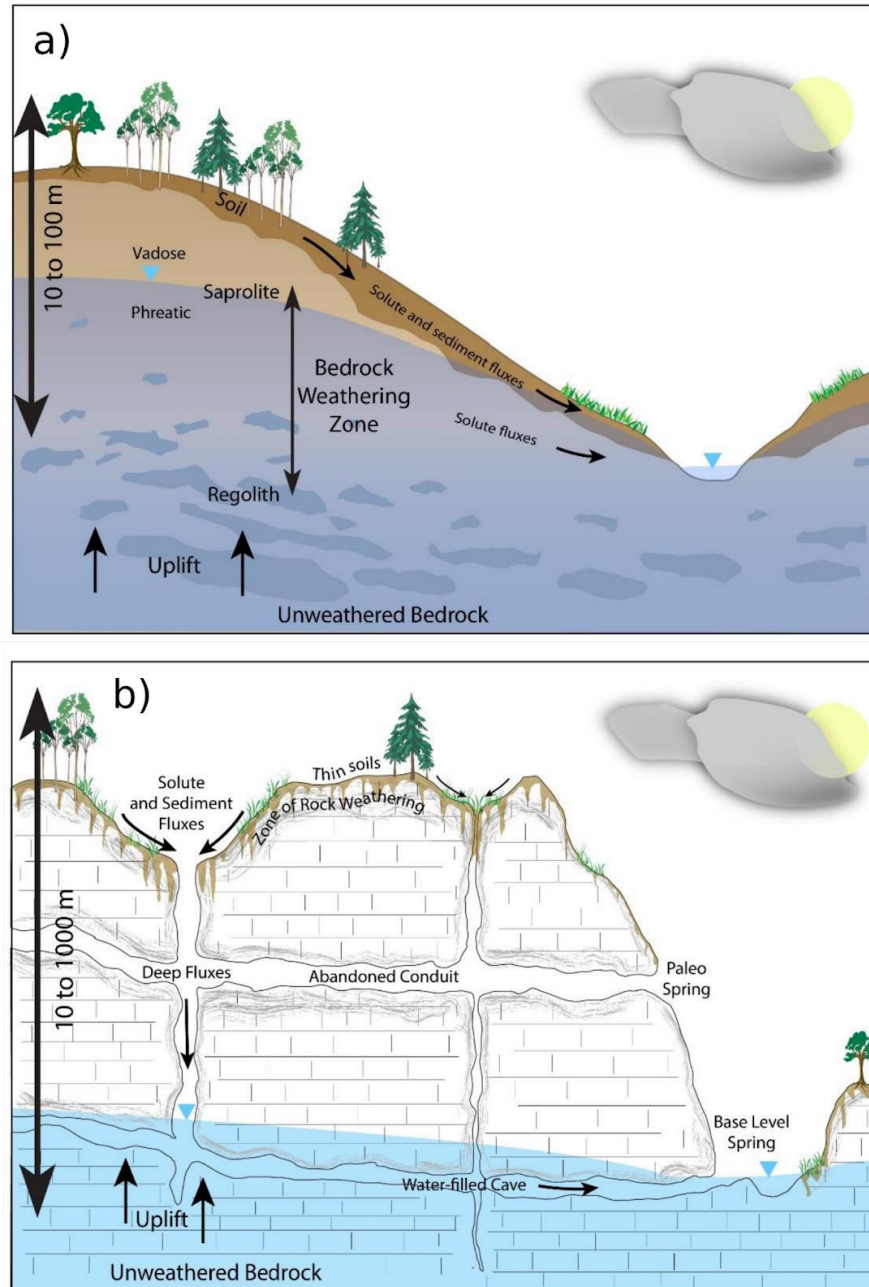
197 develop (Figure 3f). These vertical conduits capture surface runoff and route it into the  
198 subsurface. Likewise, springs are common features at contacts where confining non-carbonate  
199 rocks underlie carbonate rocks (Figure 3g). Such underlying confining units may produce a  
200 stratigraphically determined base level for the development of karst flow systems. Springs are  
201 also common where the water table intersects the land surface because erosion has removed  
202 silicate rocks and exposed high permeability zones in the underlying carbonates. Contact zones  
203 can also host estavelles (Figure 3h), features that alternate between acting as springs and sinks  
204 depending on the relative elevations of the water table and the surface water that receives spring  
205 discharge. When the surface water level at the spring rises above the hydraulic head at an  
206 estavelle, surface water may intrude into the spring, which can aid dissolution (Gulley et al.,  
207 2011) and alter concentrations of redox sensitive solutes (Brown et al., 2019).

## 208 2.2 Differences between carbonate and silicate settings

209 We use a conceptual model central to understanding CZ evolution within silicate terrains  
210 – the CZ conveyor (see e.g., Riebe et al., 2017) – to explore differences between the CZ in  
211 carbonate and silicate endmembers. Within the CZ conveyor model (Figure 4a), minerals are  
212 brought upward toward Earth's surface via erosion, exposing them to physical, chemical, and  
213 biological gradients. These gradients drive incongruent weathering that transforms bedrock into  
214 regolith that is transported down hillslopes toward stream channels. Through the migration of  
215 knickpoints, the stream channel network communicates erosion rate changes driven by tectonics  
216 or isostasy upward to the hillslopes. As channels at the base of hillslopes experience a change in  
217 erosion rate, hillslope topography and downslope transport of regolith adjust to accommodate the  
218 change. This system reaches equilibrium when fluxes of fresh rock into the CZ are balanced by  
219 fluxes of solutes and sediments out of the channel network, resulting in a steady soil and regolith  
220 thickness. This conceptual model, in various forms, is ubiquitous throughout CZ studies  
221 (Amundson et al., 2007; Anderson et al., 2013, 2002; Brantley et al., 2017a; Heimsath et al.,  
222 2020; Hilley et al., 2010; Lebedeva et al., 2010; Patton et al., 2018; Rempe and Dietrich, 2014;  
223 Riebe et al., 2017).

### 224 2.2.1 The Conveyor model and CZ architecture

225 Arguably the most fundamental difference between the weathering of silicates and  
226 carbonates is that carbonate minerals weather congruently, while silicate minerals weather  
227 incongruently. Incongruent weathering provides a key aspect of the conveyor model, whereby  
228 only a portion of the rock is removed in solution and the remaining solid mineral phases are  
229 transported to channels via hillslope processes (Figure 4a). This model thus predicts dynamic  
230 adjustment of soil and regolith thickness, producing negative feedback that drives soil production  
231 and rock lowering toward the average landscape erosion rate. When erosion rates increase, the  
232 down cutting of channels steepens the hillslopes and thins the soils, accelerating soil production.  
233 When erosion rates decrease, reduction in the rate of stream incision leads to reduction in  
234 hillslope relief, accumulation of soil, and reduction of weathering rates exponentially with soil  
235 thickness (Heimsath et al., 1997).



236  
237  
238  
239  
240  
241  
242  
243  
244  
245  
246  
247  
248

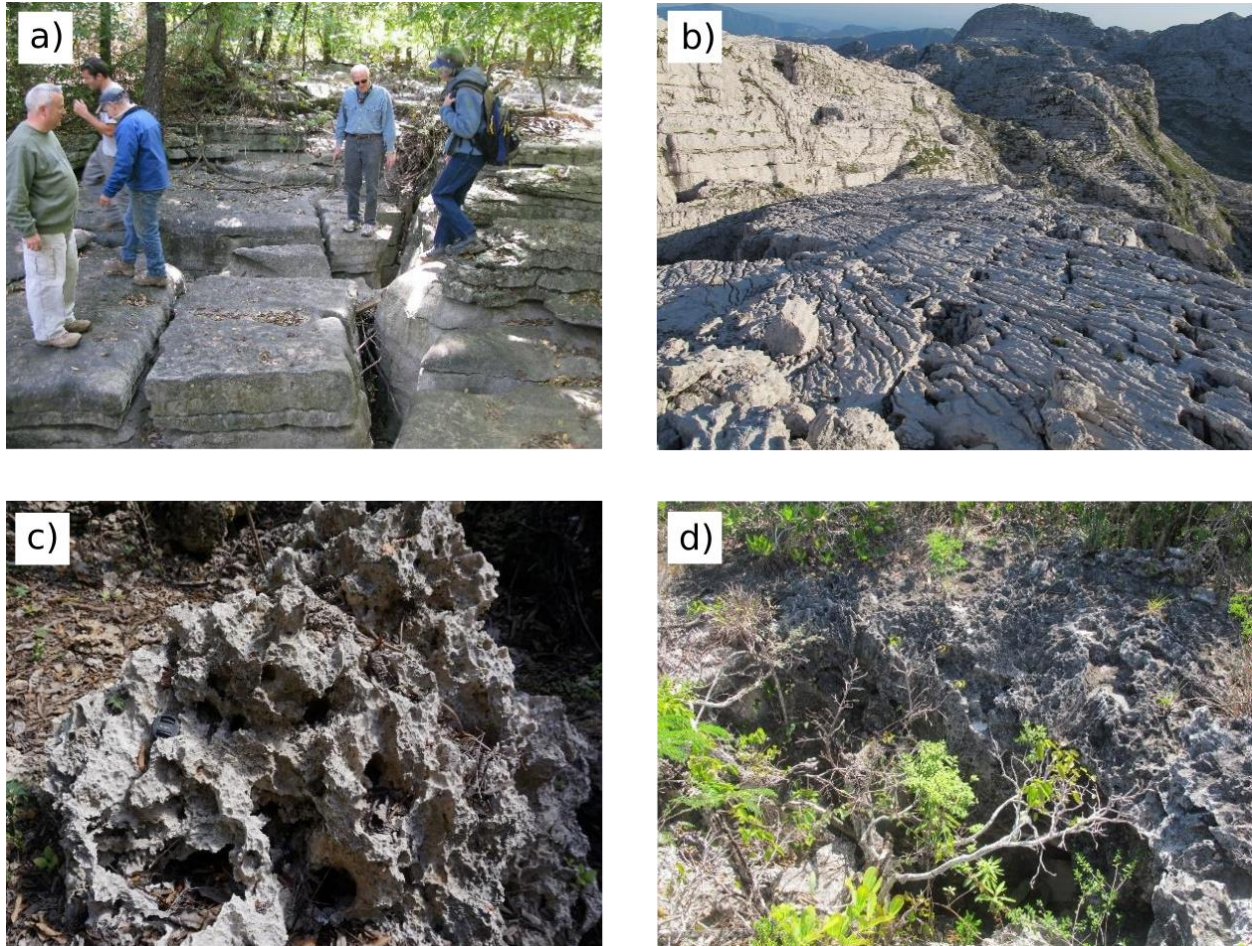
**Figure 4.** Carbonates and the conveyor model of the CZ. a) The conveyor model of the CZ, whereby uplift brings unweathered bedrock toward the surface. Weathering processes convert the bedrock into regolith and soil. Gravity transports sediment down the hillslopes, and stream channels carry away the solutes and sediments that are the byproducts of weathering. Communication between the hillslopes and channel network enables equilibration of the landscape to a rate of steady base level fall. b) Conceptual model of a well-developed karst in a carbonate setting. Surface drainage is limited. Congruent weathering of the carbonate rock leaves behind a thin soil. Much of the residuum from carbonate weathering may be routed through internally drained basins into the karst conduit network, potentially disconnecting hillslope response from changes in the rate of base level fall. Karst systems often respond to base level fall through the development of additional levels of conduits. Rapid carbonate weathering can occur deep within the subsurface in the vicinity of conduits and fractures.

249  
250  
251  
252  
253  
254  
255  
256  
257  
258  
259  
  
260  
261  
262  
263  
264  
265  
266  
267  
268  
269  
270  
271  
272  
273  
274  
  
275  
276  
277  
278  
279  
280  
281  
282  
283  
284  
285  
286  
287  
288  
289  
290  
291  
292

Unlike silicate minerals, however, congruent weathering of carbonate minerals leaves only minor amounts of insoluble residue and therefore little soil or regolith (Figure 4b). Soils in carbonate terrains may develop largely from aeolian dust deposition (Macpherson and Sullivan, 2019b), and soil thickness may depend more on the carbonate purity or dust delivery rate rather than erosion rates such as in silicate terrains (Green et al., 2019; Moore et al., 2017). Additional differences result from the greater solubility and faster reaction kinetics of carbonate than silicate minerals (Plummer et al., 1979; Svensson and Dreybrodt, 1992). Carbonate dissolution is sufficiently fast that in some cases, chemical denudation rates can outpace mechanical denudation processes (Simms, 2004), such that solute fluxes may represent the majority of the seaward flux of weathering products.

Feedback mechanisms between soil development and denudation may be weakened, or even decoupled, within pure carbonate settings, particularly if the rate of soil development is controlled by allochthonous dust input. Carbonate denudation also may be controlled more by water availability and pH, rather than by topography or soil thickness as in silicate terrains (Gabrovšek, 2009; Gombert, 2002; Ryb et al., 2014; White, 1984). The weakening of feedback between soil formation rates and denudation rates may inhibit the approach to equilibrium or at least increase the equilibration timescale. However, equilibrium configurations that are entirely internal (autogenic) are also possible. For example, biogeomorphic feedbacks between soil thickness, CO<sub>2</sub> production, and weathering rates can produce equilibrium landscapes within low relief carbonate settings, where the water table is near the surface (Cohen et al., 2011; Dong et al., 2019a, 2019b). These feedbacks produce a patterned equilibrium landscape that depends on internal controls rather than external erosional or tectonic forcing. Observations that solution doline sizes are sometimes exponentially distributed, with a characteristic scale (Troester et al., 1984; White and White, 2005), also suggests the possibility of negative feedback that may result in an autogenic equilibrium topography in other settings.

Within the conveyor belt conceptual model for the CZ, weathering occurs along planar fronts that are subparallel to the land surface (Figure 4a). In karstic carbonate terrains, weathering is focused along high permeability zones that create heterogeneous and irregular weathering patterns (Figure 4b) that are rarely subparallel to the surface (Phillips et al., 2019; Williams, 1985). Active weathering thus spans a range of depths, from exposed rock at the surface to rock that is hundreds, or even thousands, of meters below the surface (Audra et al., 2007; Klimchouk, 2019). The upper zone of weathering, often called the epikarst, typically has a higher degree of irregularity than the surface topography (Figure 5). This irregularity can grow over time through positive feedback resulting from flow-focusing (Klimchouk, 2004; Williams, 2008a, 1985) and generation of soil CO<sub>2</sub> that enhances shallow dissolution (Dong et al., 2019a; Gulley et al., 2015). The control of spatial weathering patterns in the subsurface of karst by geological structures and hydrological boundary conditions (Palmer, 1991), rather than soil properties or topography, indicates that models of carbonate CZ evolution will need to incorporate heterogeneity explicitly, as has been done in models of cave development (Dreybrodt, 1990; Gabrovšek and Dreybrodt, 2001; Groves and Howard, 1994; Hanna and Rajaram, 1998). These heterogeneities are missing from the lateral homogeneity of the conveyor belt model of the silicate CZ (Figure 4a).



293  
294  
295  
296  
297  
298  
299  
300

**Figure 5.** Weathering surfaces in carbonate terrains. a) Weathering along orthogonal joints in the St Joe Limestone in northern Arkansas. Floodwaters from a dam spillway have eroded the soil and exposed the weathering epikarst. b) Karren and epikarst surface on Dachstein Limestone on Mt. Kanin, Slovenia. c) Intense solutional weathering on an exposed piece of young, porous carbonate in Zanzibar. d) Thin soil and vegetation drape the weathering surface of young carbonates on San Salvador Island, Bahamas. In the center of the photo is the entrance of a 7-meter-deep solution shaft.

301  
302

303 The focus of dissolution along high permeability zones in carbonate terrains causes an  
304 additional breakdown of the coupling between tectonic uplift and erosion rates found in the  
305 conveyor model. In the conveyor model, surface streams transport the sediment and solutes  
306 delivered to them by hillslopes (Figure 4a), enabling landscape-wide equilibration of erosion to  
307 uplift. However, surface streams are largely absent within a mature karst terrain, as all runoff and  
308 sediment generated near the land surface is diverted into the karst conduit system through closed  
309 basins (dolines or sinkholes) (Figures 4b, 6) (Ford and Williams, 2007). Thus, if the conveyor  
310 model of the CZ is mapped from silicate to carbonate terrains, dolines would represent hillslopes  
311 and conduits would represent stream channels (Figure 4b). Even with relatively little relief (tens  
312 of meters), the hillslopes of dolines may be decoupled from base level, as dolines typically feed  
313 water and sediment vertically into the subsurface along solutionally enlarged fractures and

314 conduits (Brucker et al., 1972; Klimchouk, 2004; Palmer, 1991; Williams, 1985). Therefore,  
315 many of the “hillslopes” of karst terrains terminate at the tops of vertical subsurface channels.

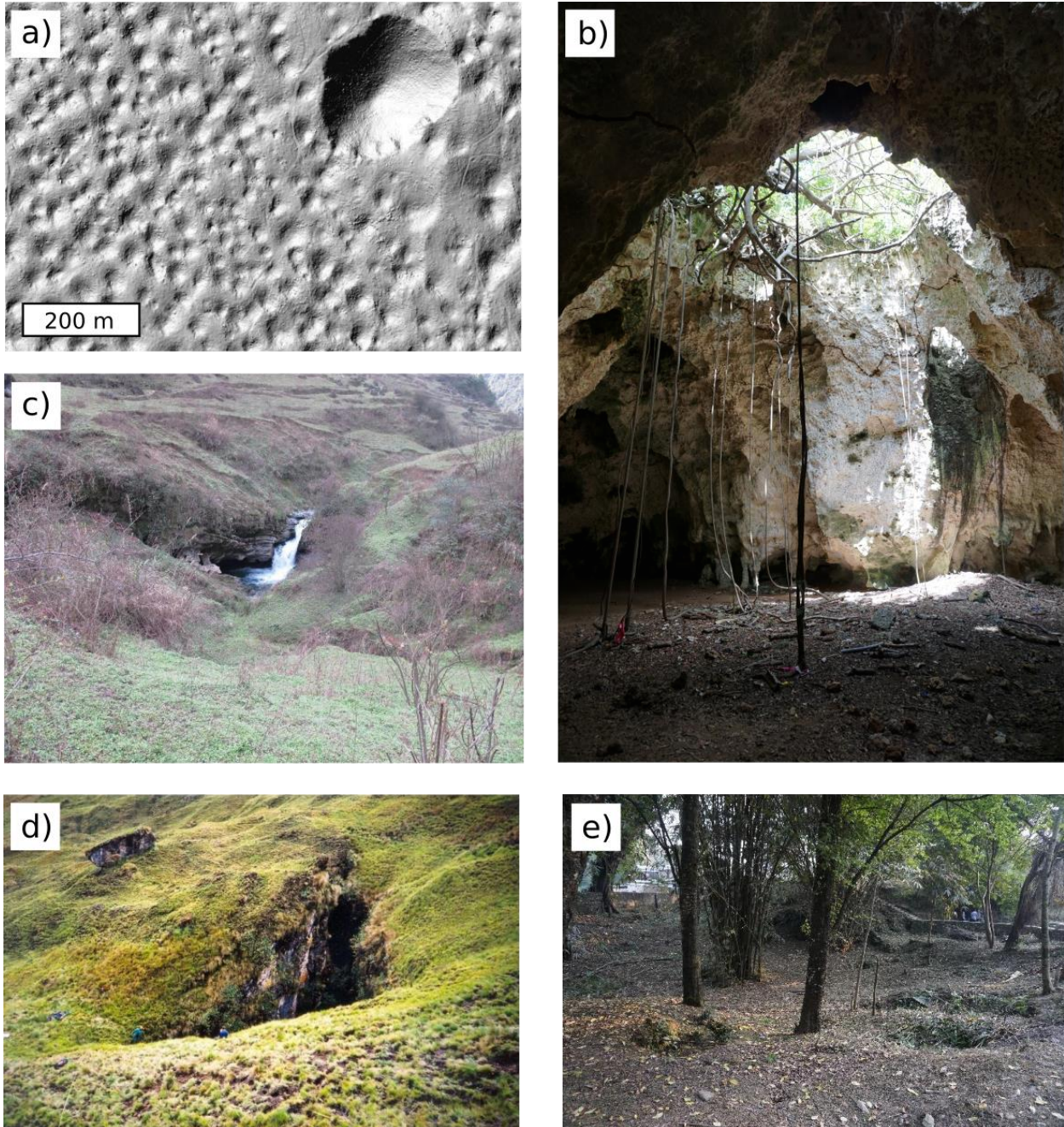
316 Even in the case of dolines feeding into subhorizontal conduits, changes at base level  
317 may not propagate through karst conduit networks as they do through surface channel networks.  
318 First, the geometry of karst conduits, including the profiles of the streams within them, are often  
319 controlled by structural heterogeneities in the rock, such as bedding partings and fractures  
320 (Filipponi et al., 2009; Lowe and Gunn, 1997; Palmer, 1991). Therefore, the initial profiles of  
321 streams within karst conduits may be far from the equivalent equilibrium channel morphologies  
322 (e.g., slope-discharge relationships) that would be expected within surface stream channels.  
323 Second, under conditions of rapid base level change, karst systems often respond by the  
324 development of new levels and abandonment of old cave channels (Figures 4b and 7) (Audra et  
325 al., 2007; Gabrovšek et al., 2014; Granger et al., 2001; Stock et al., 2005; Wagner et al., 2011),  
326 rather than through the propagation of knickpoints. Similar shifts in cave development in coastal  
327 carbonate settings result from variations in sea level (Florea et al., 2007; Gulley et al., 2013). The  
328 development of new levels within karst systems may often be sufficiently fast that stream  
329 profiles within karst conduits do not have time to adjust their long profiles and erosion rates to  
330 accommodate changes in the rate of base level rise and fall.

### 331 2.2.2 A modified conveyor model

332 The most basic concepts within the conveyor model remain intact within carbonate  
333 settings – rock is uplifted toward Earth’s surface, it undergoes weathering, and the products of  
334 weathering are transported seaward. However, the details of the conceptual model need revision  
335 in some settings. To summarize the potential differences in carbonate landscapes, we consider  
336 two modified versions of the conveyor model, which we call the “dissolving conveyor” and the  
337 “leaky conveyor.” Both modifications result in a weakening of the negative feedback  
338 mechanisms that drive weathering rates toward uplift rates and produce equilibrium landscapes,  
339 and each of these modified models relates to a dimensionless fraction (described below) that  
340 could be quantified in real landscapes.

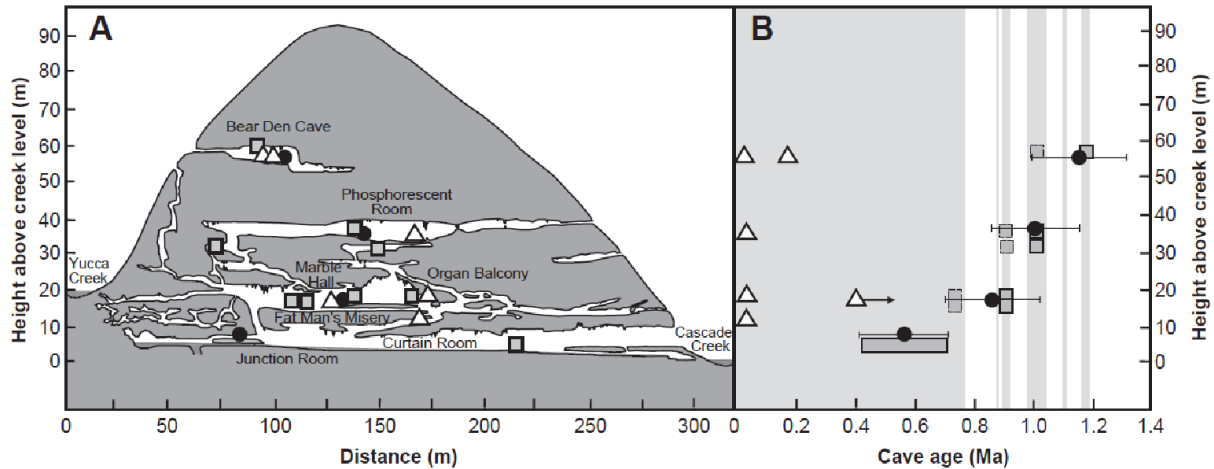
341 The dissolving conveyor describes settings where the dissolved fraction of the weathering  
342 flux is close to one, meaning that most weathered materials exit the system as solutes. In this  
343 case, the buildup of soil and regolith is insufficient to retard denudation. In cases where tectonic  
344 uplift is rapid, topography may become extremely steep, until mechanical weathering and  
345 erosion processes match uplift (Ott et al., 2019), driving the system away from the dissolving  
346 conveyor state as solid material export increases. However, in the case of low uplift, the lack of  
347 negative feedback enables the development of karst planation surfaces, because surface  
348 denudation is not arrested until the land surface approaches base level.

349 The leaky conveyor describes settings where the fraction of weathered materials  
350 transported through the karst conduit network is high, meaning that both solid and dissolved  
351 weathering materials transit through the subsurface to base level rather than down hillslopes and  
352 stream channels. Again, this weakens feedback between uplift, weathering, and erosion, as base  
353 level changes may not communicate through the subsurface. In such cases, local autogenic  
354 processes may drive patterns in topography and regolith thickness (e.g., Dong et al., 2018).  
355 While each of these modified models can be considered separately, there is likely a strong  
356 correlation between the two governing dimensionless fractions. Settings with a higher fraction of  
357 dissolved weathering fluxes will tend to have a higher percentage of weathering fluxes transiting  
358 through a conduit network.



359  
360  
361  
362  
363  
364  
365

**Figure 6.** Dolines/sinkholes and shafts in karst terrains. a) A lidar hillshade of solution dolines, and a collapse doline, on Logaška Planota, Slovenia. b) Vegetation hangs into a collapse doline in a cave system on the island of Zanzibar. c) A stream channel within a blind valley sinks into a doline near the contact with carbonate rocks in Wulong County, China. d) A 60-meter-deep vertical shaft breaches a hillslope in the Andes of northern Peru (note cavers for scale). e) Small solutional dolines developed in a calcite-cemented conglomerate near Pokhara, Nepal.



366  
367  
368  
369  
370

**Figure 7.** The development of cave levels in response to stream incision (from Stock et al., 2005). As the streams incised, new levels of cave passage were developed, rather than steepening of the existing channel, as would occur during a pulse of incision in a surface stream.

371

### 2.2.3 Soils, gases, and the silicate-carbonate spectrum

372

373

374

375

376

377

378

379

380

381

382

383

384

385

We expect that differences in soil development across the CZ silicate-carbonate spectrum will affect plant development and therefore weathering rates via plant control of carbonic acid production. Plant roots and the microbial communities they support, including mycorrhizae, saprotrophic fungi, bacteria, and archaea have long been recognized as drivers of chemical weathering and the global carbon cycle (Beerling, 1998; Berner, 1992; Brantley et al., 2017a). Plant growth elevates soil  $p\text{CO}_2$  and increases dissolved inorganic carbon (DIC) fluxes (Andrews and Schlesinger, 2001; Berner, 1997). Rooting systems (e.g., grass-, shrub- and woodlands) have been shown to govern the distribution of soil carbon (both organic and inorganic), microbial biomass, and soil respiration (Billings et al., 2018; Drever, 1994; Jackson et al., 1996). For example, relatively deep root distributions in shrublands compared to grasslands lead to deeper soil carbon profiles (Jackson et al., 1996; Jobbágy and Jackson, 2000), which elevate  $\text{CO}_2$  and therefore weathering at depth. The work described here was carried out almost exclusively at sites where the CZ is dominated by silicate minerals. Only recently have similar ideas been applied to carbonate terrains, particularly in connection with studies of land-use changes.

386

387

388

389

390

391

392

393

394

395

396

397

398

399

Changing land cover has been invoked to explain changes in carbonate weathering processes. In carbonate terrains, carbon sequestration has been found to be optimized in grasslands as compared to shrub, managed crop, soil denuded of vegetation, or bare rock dominated landscapes (Zeng et al., 2017). This optimization results from greater transformation of  $\text{CO}_2$  to DIC and greater depths of water penetration in grasslands as compared to other land cover types. However, woody vegetation encroachment into grasslands underlain by carbonate systems causes shifts in flow paths, groundwater solute concentration, and the timing of solute delivery to streams as shown by reactive transport models of observed changes in stream and groundwater chemical compositions (Sullivan et al., 2019). Deep root systems of the woody plants control thermodynamic limits of carbonate dissolution by regulating how much  $\text{CO}_2$  is transported downward to the deeper carbonate-rich zone (Wen et al., 2020). Even in karst wetland systems, the delivery of biologically derived acids into the soil zone, which is sensitive to precipitation regimes, inundation periods, vegetation characteristics, and groundwater drainage, drives where and at what depth the maximum weathering rates occur (Dong et al.,

2019a). Additionally, analysis of global datasets shows that ecosystem respiration, which to a degree is controlled by temperature, is a main driver of soil-rock  $p\text{CO}_2$  and suggests that at a global scale, carbonate soil-rock interaction can be described by an open system with respect to  $p\text{CO}_2$  (Romero-Mujalli et al., 2019). Furthermore, this same dataset demonstrated that changes in temperature and precipitation can prompt the opposite effects on soil moisture and equilibrium constants in carbonate weathering reactions, leading to the maximum rates of dissolution and soil  $\text{CO}_2$  production in temperate climates (10-15°C) (Gaillardet et al., 2019).

Bedrock type can control plant productivity through influencing the available nutrients and physical regolith structure (Hahm et al., 2014). Data from carbonate settings suggest that silicate percentage is negatively correlated with the rate of water drainage from regolith and positively correlated with primary productivity (Jiang et al., 2020). It is hypothesized that preferential drainage features are better developed within carbonate-rich rocks and that this leads to both water and regolith loss into the subsurface, reducing water availability during dry periods. Similarly, a global study of relationships between rock type and biodiversity in erosional landscapes demonstrates that regions rich in carbonates have less vegetation and lower animal richness (Ott 2020).

The importance of vadose zone gases, particularly  $\text{CO}_2$  and  $\text{O}_2$ , to weathering processes (e.g., Brantley et al., 2013; Kim et al., 2017) leads to distinct differences in weathering across the silicate-carbonate mineral spectrum of the CZ. Gases are often assumed to be transported by diffusive processes in the vadose zones of the CZ, where dominated by low permeability silicate minerals. These gases are derived from Earth's atmosphere as a primary source (Kim et al., 2017; Wood and Petraitis, 1984). However, connectivity among solutionally enlarged fractures and larger conduits in karst systems enables advective gas flows. Advection is forced by density contrasts between surface and subsurface air, largely through temperature variations at daily and seasonal time scales (Covington, 2016; Sanchez-Cañete et al., 2011), that drive seasonal and diurnal changes in subsurface gas concentrations (Benavente et al., 2010; Gulley et al., 2014; Kowalczk and Froelich, 2010; Lang et al., 2017; Matthey et al., 2016; Milanolo and Gabrovšek, 2009; Spötl et al., 2005; Wong et al., 2011). These variations are likely to extend throughout the vadose zone, even where it may be thick because of deep groundwater tables (Benavente et al., 2010; Covington, 2016; Matthey et al., 2016). In some cases, soil and the shallow subsurface may be aerated from below rather than directly from the atmosphere (Faimon et al., 2020). The ventilation through conduit systems, and the linked changes in vadose water chemical compositions and compositions at the water table, can thus provide controls on the spatial and temporal patterns of dissolution and precipitation of calcite (Covington et al., 2021; Covington and Vaughn, 2019; Gulley et al., 2014; Houillon et al., 2017; Spötl et al., 2005; Wong et al., 2011).

### 2.3 How deep is the CZ?

The dissolutional enhancement of permeability, and the resulting high flow velocities (Worthington et al., 2016), produce rapid advection of solutes into the subsurface. After development of preferential flow paths, substantial changes in flow and chemistry can be expected deep within and throughout the carbonate CZ over short time periods, such as individual storm events. Such variability is expected both within larger dissolutional conduits (e.g., Ashton, 1966; Birk et al., 2006; Brown et al., 2014; Covington et al., 2012; Groves and Meiman, 2005; Gulley et al., 2011; Liu et al., 2004; Vesper and White, 2004) and within smaller dissolutionally enlarged fractures and the epikarst (Kogovšek and Petrič, 2012; Liu et al., 2007; Miorandi et al., 2010; Musgrove and Banner, 2004; Tooth and Fairchild, 2003). Consequently,

446 within the carbonate CZ, surface-like geochemical conditions can occur at substantial depth and  
447 at long distances from locations of point recharge. These changes deep within the carbonate CZ  
448 differ from the commonly assumed base of the silicate CZ as the depth where regolith formation  
449 begins (Figure 4). Thus, an important consideration in contrasting Earth's CZ in endmember  
450 carbonate and silicate settings lies in the definition of the CZ itself, specifically, its lower  
451 boundary, and the lower boundary's relationship with the mineralogical makeup of the CZ and  
452 active circulation of water (Condon et al., 2020).

453 Riebe et al. (2017) review possible criteria for defining the base of the CZ. Ultimately,  
454 they settle on an equilibrium-based definition, that is, the base of the CZ is the depth in the  
455 subsurface at which meteoric water and Earth materials are at chemical equilibrium. Although  
456 they do not explain why, they also note that a different definition may be needed for carbonate  
457 settings. We see two ways in which the equilibrium definition might be problematic in  
458 carbonates. First, given that active dissolution of calcite by meteoric water can occur at great  
459 depths, up to thousands of meters (Klimchouk, 2019), the lower boundary using this definition  
460 can be quite deep, leading to a picture of the CZ that differs substantially from the typical  
461 hillslope catena (Figure 4). However, given that deep karst conduits can provide important  
462 controls on the fluxes of water, gas, and sediment through the CZ, it seems that a holistic  
463 understanding of the carbonate CZ requires an incorporation of coupling between the near and  
464 deep subsurface. Therefore, the extreme depth of carbonate dissolution illustrates a meaningful  
465 difference in the dynamics and processes that occur in carbonate and silicate settings.

466 Perhaps ironically, the second potential problem that we can see with the equilibrium  
467 definition of the base of the carbonate CZ is that, due to rapid kinetics, meteoric water  
468 equilibrates quickly with carbonates. Consequently, water may be effectively saturated with  
469 calcite in the near subsurface, ending further chemical weathering. That is, the equilibrium  
470 definition may specify too shallow a depth of the CZ, with a bottom boundary that is above  
471 depths in which additional CZ processes occur. In fact, these two problems can be seen as  
472 opposite sides of the same coin. They both result from the non-planar nature of the weathering  
473 front within carbonates (Phillips et al., 2019). Although meteoric water often comes close to  
474 equilibrium with calcite in the near subsurface, non-linear kinetics reduce dissolution rates as  
475 water nears equilibrium with carbonate minerals, enabling undersaturated water to penetrate deep  
476 into the subsurface (Dreybrodt, 1990; Palmer, 1991). Even in the absence of such non-linear  
477 kinetics, flow fingering or "wormhole" development can drive undersaturated water deep into  
478 dissolving fractures (Szymczak and Ladd, 2011, 2012). Additionally, dissolutional capacity can  
479 be added to alter equilibrium conditions in the deep subsurface by many processes. These  
480 processes include CO<sub>2</sub> production (Atkinson, 1977b; Benavente et al., 2010; Gulley et al., 2015;  
481 Matthey et al., 2016), mixing of surface-derived meteoric water with water containing H<sub>2</sub>S (Davis,  
482 1980; Egemeier, 1987; Hill, 1990; Jagnow et al., 2000; Palmer, 1991; Martin, 2017), mixing of  
483 water with different partial pressures of CO<sub>2</sub> (Bögli, 1964; Wigley and Plummer, 1976), or  
484 mixing with salt water (Back et al., 1986; Mylroie and Carew, 1990; Plummer, 1975). Each of  
485 these processes may alter the equilibrium conditions deep within the CZ.

486 Despite potential difficulties outlined above, we think that an equilibrium-based  
487 definition of the lower boundary of the CZ in carbonates is a reasonable starting point. A  
488 working definition of the base of the CZ in carbonate settings would then be, "The depth below  
489 which there is no measurable dissolution of carbonate minerals by meteoric water." This  
490 definition comes with the caveats that: 1) much of the water between the surface and the base of  
491 the CZ will be near equilibrium with respect to carbonate minerals, and 2) some of the  
492 dissolution will be driven by subsurface acid production and/or mixing of meteoric water with

493 deeper water. Perhaps the most difficult delineation to make is between dissolution processes  
494 that are driven by proximity to Earth's surface and those which can occur at great depth from  
495 rising thermal waters, H<sub>2</sub>S-rich fluids, or volcanic production of CO<sub>2</sub>. While many of these  
496 deeper processes may create a template for further permeability development by near-surface  
497 processes as rocks are exhumed, they can be considered as initial conditions for CZ  
498 development, much like the initial mineralogy, fabric, and structures of the exhumed rock layers,  
499 rather than an integral component of CZ processes. Here, we propose that dissolution processes  
500 that should be considered to define the bottom boundary of the CZ are those that produce  
501 feedback with the near-surface hydrological, geomorphological and biogeochemical processes,  
502 such that the dissolution processes both influence and are influenced by the flow of meteoric  
503 water.

### 504 **3. The variety of carbonate CZ settings**

505 In the previous section, we explored the carbonate-silicate spectrum (Figure 2), where  
506 both the percentages and distributions of silicate and carbonate minerals impact CZ development  
507 and result in distinctly different CZ characteristics, processes, and material fluxes. Within  
508 carbonate terrains, geological, hydrological, biological, geochemical, and climate variables  
509 produce a broad array of carbonate CZ characteristics. Here, we explore the range of parameters  
510 that create important differences within the carbonate CZ.

#### 511 3.1 The importance of porosity distributions

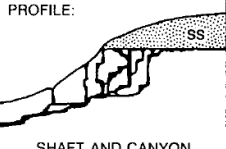
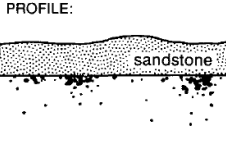
512 Where the CZ occurs in nearly pure carbonate terrains, it is often transformed through  
513 congruent dissolution into karst (Ford and Williams, 2007). Most karst landscapes form in  
514 carbonate bedrock, because of its common occurrence, although they also develop in evaporites  
515 (Klimchouk et al., 1996; Frumkin, 2013) and occasionally, in less soluble rocks (Wray and  
516 Sauro, 2017). Carbonate rocks tend to form karst because of their high solubility and rapid  
517 dissolution rates. Dissolution integrates subsurface flow networks as water penetrates along  
518 heterogeneities in the rock and links input to outpoint points (Dreybrodt, 1990; Ford et al., 2000;  
519 Palmer, 1991). Such integrated flow paths, or karst conduits, are characterized by elevated  
520 permeability and exhibit rapid and turbulent flow that transports large quantities of solutes and  
521 gases between the surface and subsurface. High flow rates also allow the conduits to transport  
522 sediment through the subsurface (Cooper and Covington, 2020; Farrant and Smart, 2011;  
523 Herman et al., 2012). Once the capacity of the subsurface conduit network is sufficient to carry  
524 available surface runoff and sediment, closed basins develop on the land surface that route water  
525 and sediment into the subsurface. Conduit systems exit at springs, which frequently develop near  
526 the local hydrological base level. Together, these processes lead to the dolines, caves, and  
527 springs that characterize karst landscapes.

528 Karst aquifers are commonly conceptualized as a triple-porosity system, in which  
529 porosity is divided into a matrix component, a fracture component, and a conduit component  
530 (Quinlan et al., 1996; White, 2002; Worthington, 1999). The matrix component represents the  
531 primary porosity of the bedrock. The fracture component represents secondary porosity as a  
532 result of fractures and bedding partings. The conduit component represents dissolutionally  
533 enlarged flow paths that have increased connectivity as a result of positive feedback between  
534 dissolution and flow focusing (Worthington et al., 2016). While the dividing line between  
535 conduits and fractures is somewhat arbitrary, often the conduits are defined as the flow paths that  
536 carry turbulent flow (White, 2002). The three porosity components differ in their ability to store  
537 and transmit water. Primary porosity provides much more storage than the conduit network,

538 because of its large total volume, whereas conduits transmit the most water, because of their high  
539 permeability (Worthington, 1999). These different hydrologic characteristics create a scale-  
540 dependent hydraulic conductivity in karst aquifers. Hydraulic conductivity over short distances is  
541 controlled by the primary porosity and is thus relatively low. Hydraulic conductivity increases  
542 over intermediate distances as fractures become important and is greatest at aquifer scales where  
543 flow through conduits dominates (Halihan et al., 2000; Király, 1975; Worthington, 2009).

544 The primary porosity within a carbonate rock is a function of its diagenetic history and  
545 whether the rock has undergone burial diagenesis, which dramatically reduces primary porosity.  
546 The terms eogenetic karst and telogenetic karst are used to distinguish karst that is developed  
547 within relatively young carbonates that have primarily undergone meteoric (eogenetic)  
548 diagenesis from karst developed in older carbonates that have experienced burial diagenesis  
549 (telogenetic) and re-exposure to the surface via erosion (Vacher and Myroie, 2002; Choquette  
550 and Pray, 1970). Integrated karst flow networks develop most easily in rocks with relatively low  
551 primary porosity and relatively high fracture porosity (Palmer, 1991; White, 1969; Worthington,  
552 2014). Such conditions focus flow through higher permeability fractures, increasing flow  
553 velocities and the depth to which undersaturated water can penetrate the rock, ultimately leading  
554 to breakthrough of dissolutionally enlarged pathways that connect inlets to outlets (Dreybrodt,  
555 1990). Positive feedback focuses flow, whereby the most efficient flow paths receive the most  
556 flow and therefore grow most rapidly, diverting even more flow into these pathways and further  
557 accelerating their growth (Ewers, 1982; Palmer, 1991; Siemers and Dreybrodt, 1998). The  
558 largest developing flow paths create troughs in the potentiometric surface, such that other  
559 competing pathways are drawn toward them, frequently producing a dendritic pattern like that  
560 found in surface stream networks. The overall conduit network geometry is strongly influenced  
561 by the nature of recharge to the aquifer and the locations of recharge and outlet points (Figure 8)  
562 (Palmer, 1991).

563

|                           |                            | TYPE OF RECHARGE   |  |  |   |  |  |   |  |
|---------------------------|----------------------------|--|--|--|---|--|--|---|--|
|                           |                            | VIA KARST DEPRESSIONS  |  | DIFFUSE  |   | HYPOGENIC  |  |   |  |
|                           |                            | SINKHOLES<br>(LIMITED DISCHARGE<br>FLUCTUATION)              | SINKING STREAMS<br>(GREAT DISCHARGE<br>FLUCTUATION)  | THROUGH SANDSTONE  | INTO POROUS<br>SOLUBLE ROCK                                     | DISSOLUTION BY ACIDS OF<br>DEEP-SEATED SOURCE OR<br>BY COOLING OF THERMAL<br>WATER |  |   |  |
| DOMINANT TYPE OF POROSITY |                            | BRANCHWORKS<br>(USUALLY SEVERAL LEVELS)<br>& SINGLE PASSAGES |  | SINGLE PASSAGES AND<br>CRUDE BRANCHWORKS,<br>USUALLY WITH THE<br>FOLLOWING FEATURES<br>SUPERIMPOSED: |   | MOST CAVES ENLARGED<br>FURTHER BY RECHARGE<br>FROM OTHER SOURCES                   |  | MOST CAVES FORMED BY<br>MIXING AT DEPTH |  |
| FRACTURES                 | ANGULAR<br>PASSAGES        | FISSURES,<br>IRREGULAR NETWORKS                              | FISSURES, NETWORKS   | ISOLATED FISSURES<br>AND RUDIMENTARY<br>NETWORKS   | NETWORKS,<br>SINGLE PASSAGES, FISSURES                          |  |  |   |  |
|                           | CURVILINEAR<br>PASSAGES    | ANASTOMOSES,<br>ANASTOMOTIC MAZES                            | PROFILE:<br>  | SPONGEWORK   | RAMIFORM CAVES,<br>RARE SINGLE-PASSAGE AND<br>ANASTOMOTIC CAVES |  |  |   |  |
|                           | RUDIMENTARY<br>BRANCHWORKS | SPONGEWORK   | PROFILE:<br> | SPONGEWORK   | RAMIFORM & SPONGEWORK<br>CAVES                                  |  |  |   |  |

564  
565 **Figure 8.** Relationship between recharge, dominant porosity, and the patterns of karst networks  
566 that develop (from Palmer, 1991).

567  
568

569       Rocks with high primary porosity, as found in eogenetic karst, preferentially develop  
570 spongework caves (Palmer, 1991), which are often isolated voids that are not connected into an  
571 integrated conduit flow system (Vacher and Mylroie, 2002). Examples of such dissolutional  
572 voids include the flank margin caves and “banana holes” that develop in carbonate island karst  
573 (Breithaupt et al., 2021; Mylroie and Carew, 1990; Vacher and Mylroie, 2002). In such settings,  
574 the locations of dissolutional voids may be controlled by zones of mixing (Mylroie and Carew,  
575 1990) or by biological CO<sub>2</sub> production (Gulley et al., 2016, 2015). Consequently, voids  
576 frequently develop near the water table, where vadose zone CO<sub>2</sub> can boost dissolution rates  
577 (Gulley et al., 2014), or in zones of freshwater-saltwater mixing (Mylroie and Carew, 1990).  
578 While evolution of such voids produced by local mixing or CO<sub>2</sub> production may enhance local  
579 hydraulic conductivity and focus porous media flow toward enlarging voids (Mylroie and Carew,  
580 1990; Vacher and Mylroie, 2002), it is less common for these processes to develop regionally  
581 integrated conduit systems (Palmer, 1991). However, long-range conduit connectivity can still  
582 develop in eogenetic karst, particularly in the case of sinking streams (Martin and Dean, 2001;  
583 Monroe, 1976), reversing springs (Gulley et al., 2011), or large recharge areas as found in the  
584 Yucatan Peninsula of Mexico (Back et al., 1986) and on large carbonate islands (Larson and  
585 Mylroie, 2018).

586 The primary porosity of carbonate rocks also impacts the magnitude of water exchange  
587 between conduits and the porous matrix. The matrix component is often considered negligible in  
588 models of flow and transport in telogenetic karst aquifers (Peterson and Wicks, 2005). However,  
589 in eogenetic karst, with high matrix porosity, transient head conditions within conduits,  
590 combined with the relatively high permeability of the matrix, can produce substantial exchange  
591 flows between the conduits and matrix, analogous to hyporheic exchange within rivers (Martin  
592 and Dean, 2001). Such exchange flows may dampen the hydraulic response of karst aquifers,  
593 which are typically flashy (Florea and Vacher, 2006; Spellman et al., 2019). The loss of water  
594 from large void spaces making up conduits to small intergranular matrix porosity increases  
595 surface areas available for dissolution reactions. In some cases, dissolution by exchange flow  
596 may be the primary factor driving evolution of connectivity within a karst aquifer (Gulley et al.,  
597 2011). Exchange flows are also important drivers of a variety of other biogeochemical reactions,  
598 in large part because of their control of redox condition as water equilibrated with atmospheric  
599 oxygen and elevated in dissolved organic carbon is injected into reducing water stored in matrix  
600 porosity (Brown et al., 2014; 2019; Flint et al., 2021). Such exchange flows can occur both  
601 between conduits and matrix and between rivers and the surrounding aquifer.

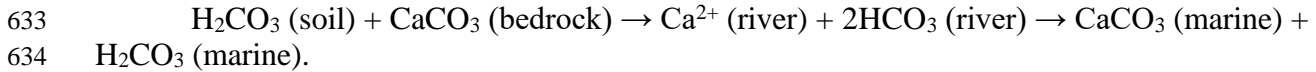
### 602 3.2 The source of undersaturation and dissolution

603 In the classic conceptual model of karst development, calcite dissolution is driven by  
604 carbonic acid. Meteoric water dissolves CO<sub>2</sub> within the soil and carries this CO<sub>2</sub> downward into  
605 the rock, dissolving carbonate minerals along its way. Karst developed by such processes is often  
606 referred to as epigene karst, indicating its close relationship to surface processes. This classic  
607 conceptual model has been expanded in a number of ways, particularly as relates to the sources  
608 of CO<sub>2</sub>. In some karst settings, CO<sub>2</sub> concentrations are higher at depth than within the soil,  
609 suggesting CO<sub>2</sub> production deep within the vadose zone, perhaps as the result of the  
610 remineralization of particulate organic matter that has infiltrated to depth (Atkinson, 1977b;  
611 Matthey et al., 2016; Wood, 1985).

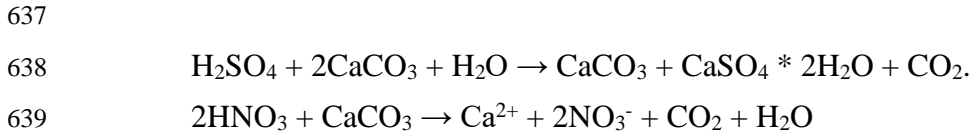
612 In addition to carbonic acid, carbonate dissolution can be driven by a variety of other  
613 acids, with sulfuric and nitric acids being the most common. Sulphuric acid is widely cited as a  
614 source of dissolution in hypogenic speleogenesis (Egemeier, 1988; Engel et al., 2004), in marine  
615 carbonate sediments (Beaulieu et al., 2011; Torres et al., 2014), and in landscapes affected by  
616 acid rain (Shaughnessy et al., 2021). Sulphuric acid can be produced through fossil fuel  
617 combustion, especially coal (Irwin and Williams, 1988). Sulfuric acid is also produced where  
618 oxygen-rich air or water encounters reduced sulfur species such as pyrite in sedimentary rocks or  
619 H<sub>2</sub>S produced by coupled microbial organic carbon oxidation and sulfate reduction. Carbonate  
620 dissolution can also occur by nitric acid produced during microbial nitrification or industrial  
621 processes. Nitric acid production has been enhanced by anthropogenic production of reactive  
622 nitrogen species (Galloway, 1998; Galloway et al., 2008), for example by chemical fertilizer use  
623 in intensive agriculture and partial oxidation of atmospheric N<sub>2</sub> in internal combustion engines  
624 (Gandois et al., 2011; Perrin et al., 2008). Organic acids may also be important drivers of  
625 dissolution in some carbonate settings although their concentrations are commonly lower than  
626 concentrations of sulfuric or nitric acids (Jones et al., 2015). High concentrations of organic  
627 acids have been observed to cause rapid carbonate dissolution in a temperate rainforest setting  
628 (Allred, 2004; Groves and Hendrikson, 2011).

629 The source and type of acid causing carbonate dissolution is critical to global carbon  
630 cycling (Martin, 2017). Carbonate dissolution by carbonic acid is neutral with respect to long-

631 term atmospheric CO<sub>2</sub> concentrations, because CO<sub>2</sub> consumed during weathering is balanced by  
 632 CO<sub>2</sub> released during marine carbonate precipitation, with



635 In contrast, dissolution of carbonates by sulfuric or nitric acids results in a net flux of  
 636 CO<sub>2</sub> to the atmosphere (Martin, 2017), with



640  
 641 Considerable work over the last two decades has focused on hypogene speleogenesis, in which  
 642 water undersaturated with respect to bedrock minerals forms at depth and is carried to the surface  
 643 with regional groundwater flow (Klimchouk, 2007; Palmer, 1991). Undersaturated water may  
 644 form through many mechanisms, including cooling of rising thermal waters, oxidation of  
 645 reduced sulfur species, deep sources of CO<sub>2</sub>, and mixing of waters with different salinity or  
 646 *p*CO<sub>2</sub>. Dissolution deep within a karst aquifer may develop porosity that is disconnected from  
 647 points of surface recharge, forming isolated porosity rather than regionally integrated flow  
 648 networks. Alternatively, dissolution where deep and meteoric water mix may develop integrated  
 649 flow networks if the pore spaces become linked. Karst conduit networks formed by hypogene  
 650 processes typically develop complex mazes or ramiform passages, with less tendency toward the  
 651 dendritic flow patterns common in epigene karst settings (Palmer, 1991). Porosity that develops  
 652 in the deep subsurface may serve as a template for epigenetic karst processes when exhumation  
 653 due to erosion brings that porosity closer to the surface (e.g., Tennyson et al., 2017).

### 654 3.3 Climatic gradients

655 Climatic factors impact the rates and forms of karst development (Lehmann, 1936). A  
 656 theoretical relationship for the maximum possible rates of karst denudation ( $D_{\max}$ ) based on  
 657 equilibrium carbonate chemistry (White, 1984) provides a first order estimate of the impact of  
 658 climate factors on rates of carbonate denudation,

$$659 \\ 660 \quad D_{\max} = \frac{100}{\rho} \left( \frac{K_c K_1 K_{\text{CO}_2}}{K_2} \right)^{\frac{1}{3}} p\text{CO}_2^{\frac{1}{3}} (P - E) \quad (1)$$

661 where  $\rho$  is rock density,  $K_c$ ,  $K_1$ ,  $K_{\text{CO}_2}$  and  $K_2$  are equilibrium constants of the carbonate system,  
 662  $p\text{CO}_2$  is the partial pressure of CO<sub>2</sub>, and  $P - E$  is precipitation minus evapotranspiration.  
 663 Equation 1 shows the three main contributors to climate-driven differences in carbonate  
 664 denudation rates: 1) temperature-dependent changes in the equilibrium constants, 2) differences  
 665 in  $p\text{CO}_2$ , which are strongly related to temperature, and 3) water availability. Among these three  
 666 factors, water availability plays the strongest role in producing global variation in chemical  
 667 denudation rates (Ryb et al., 2014; Smith and Atkinson, 1976). Well-developed karst surface  
 668 features are less common within hot and arid settings or cold settings where water is rarely  
 669 present in a liquid state (Ford and Williams, 2007). When karst surface features are present in  
 670 such settings, they are sometimes inherited from landscapes that developed in past conditions  
 671 that were wetter.  
 672

673 As temperature increases, solubility of calcite decreases, largely because of the decreased  
674 solubility of CO<sub>2</sub>. However, carbonate mineral dissolution rates increase with warmer  
675 temperatures (Plummer et al., 1978). Elevated dissolution rates decrease the time required to  
676 reach equilibrium within the critical zone and thus faster kinetics lead to more dissolution within  
677 the near subsurface (Gabrovšek, 2009). In addition, soil *p*CO<sub>2</sub> increases with increased  
678 temperature as biological activity increases. These two competing effects are thought to produce  
679 the observed boomerang shape between Ca<sup>2+</sup> + Mg<sup>2+</sup> concentrations and temperature within  
680 world rivers, which suggests carbonate weathering intensity peaks around a temperature of 10 C  
681 (Gaillardet et al., 2019). While a substantial body of work examines fluxes of solutes from  
682 carbonate basins and uses these to estimate average denudation rates, the role of kinetics in  
683 partitioning dissolution within the subsurface remains an area for further study.

684 Climate, represented by the combination of water availability and temperature, has a  
685 strong impact on the types of ecosystems present within different carbonate settings. Given the  
686 close ties between biological CO<sub>2</sub> production and carbonate weathering, climate will indirectly  
687 influence patterns and rates of carbonate weathering through its influence on biological  
688 processes. The obvious first order effect is that warmer environments lead to higher rates of soil  
689 and root respiration and therefore higher *p*CO<sub>2</sub> in the subsurface (Drake, 1980). Climate can  
690 create feedbacks between biological, hydrological, and geomorphological processes to produce  
691 patterned landscapes within carbonate settings (Dong et al., 2019b), but other interactions  
692 between climate and karst landscape development are not well-understood. For example,  
693 polygonal or cockpit karst develops preferentially in the humid tropics, whereas doline karst is  
694 more typical of humid temperate regions, and the reason for this difference is unclear (Ford and  
695 Williams, 2007). Similar to the development of patterned karst landscapes, biological processes  
696 may be an important driver in the evolution of these landscapes.

### 697 3.4 Tectonic setting and base level

698 Tectonic uplift, sea level change, and other drivers of changes in base level provide  
699 important boundary conditions for the development of karst flow networks and the resulting  
700 landscapes. Karst conduit development is often focused near the water table. During periods of  
701 stable base level, karst conduit networks can preferentially develop within specific elevation  
702 ranges (Figures 4b and 7). Such cave levels are used to date phases of river incision using  
703 cosmogenic burial dating (Granger et al., 2001; Stock et al., 2005). Similarly, flat corrosion  
704 plains develop when the land surface approaches base level (Ford and Williams, 2007). In  
705 contrast, where rapid uplift occurs, the resulting high relief promotes the development of thick  
706 vadose zones, sometimes in excess of 2 km. In these cases, conduit development may be  
707 primarily vertical, along structural features such as faults, until water collects within  
708 subhorizontal conduits that drain the water laterally out of massifs into springs near base level  
709 (Audra et al., 2006; Turk et al., 2014; Klimchouk, 2019). Uplift of carbonate platforms can also  
710 result from isostatic rebound caused by dissolution and the resulting reduction in platform  
711 density (Adams et al., 2010; Opdyke et al., 1984). In fold and thrust belts, the tendency for  
712 evaporites to act as planes of detachment frequently results in the formation of anticlines with  
713 evaporite cores (Davis and Engelder, 1985), and the buoyant effect of the evaporites may be an  
714 additional force contributing to uplift of the anticline (Lucha et al., 2012). The juxtaposition of  
715 evaporites below uplifted, fractured carbonate-rich rocks creates ideal conditions for hypogene,  
716 sulfidic karst development, as in the Central Apennines, Italy (D'Angeli et al., 2019). In this  
717 setting, base level is controlled by river incision of the anticline, resulting in sulfidic springs that  
718 discharge in or near river valleys. Cycles of sea level rise and fall are important drivers of karst

719 development in coastal settings, which are typical of most eogenetic karst. Voids that develop at  
720 sea-level low stands are subsequently flooded during sea level rise (Myroie and Carew, 1990;  
721 Smart et al., 2006; Gulley et al., 2013).

### 722 3.5 Relative importance of chemical vs. mechanical weathering processes

723 Landscapes that develop on carbonate bedrock are impacted by the types and rates of  
724 mechanical weathering and erosion. In landscapes where mechanical processes are more efficient  
725 than chemical processes, karst features will be less pronounced, even if subsurface karst flow  
726 networks are well-developed. The instantaneous rate of chemical erosion tends to be slower than  
727 the instantaneous rates of mechanical erosion processes such as bedrock abrasion, hillslope mass  
728 wasting, and glacial erosion. Chemical erosion processes are often relatively continuous, with  
729 chemical denudation rates depending primarily on climate (White, 1984) and dissolution rates  
730 within streams showing relatively low variability over time (Covington et al., 2015). In contrast,  
731 mechanical erosion and mass transport processes are frequently episodic. Consequently, the most  
732 extensive karst landscapes develop in humid environments where nearly continuous chemical  
733 weathering outpaces episodic mechanical processes – a tortoise and hare analogy (Simms, 2004).  
734 In environments where mechanical weathering processes are particularly effective, karst surface  
735 features may fail to develop because of the rapid breakup and accumulation of weathered rock.  
736 One such example is alpine karst settings, where frost cracking can erase surface expressions of  
737 karst (Ford, 1971).

738 In mixed carbonate and non-carbonate terrains, carbonates can behave either as weaker  
739 rock layers, forming topographic lows, or as strong layers that form topographic highs (Simms,  
740 2004; Ott et al., 2019). When chemical weathering rates outpace tectonic uplift, as might be the  
741 case in either humid environments or tectonically passive settings, then carbonates tend to erode  
742 more quickly and develop lows in the topography. However, when tectonic uplift outpaces  
743 chemical weathering, as in arid or rapidly uplifting environments, then the mechanical strength  
744 of carbonates may result in the formation of topographic highs (Ott et al., 2019).

745 The diversion of surface water, and therefore geomorphic work, into the subsurface in  
746 sinking streams can influence the efficiency of fluvial erosion processes. For example, karst sink  
747 points can stall the propagation of knickpoints, reducing rates at which stream profiles adjust to  
748 changes in tectonic forcing (Fabel et al., 1996). Ott et al., (2019) quantified both chemical and  
749 mechanical erosion rates in carbonates and non-carbonates in Crete, showing that mechanical  
750 erosion processes dominate, even in the carbonates, where chemical denudation accounts for  
751 ~40% of total erosion. Their results suggest that the much greater relief that develops in the  
752 carbonates results from loss of water into the subsurface and subsequent steepening of stream  
753 channels to enable mechanical erosion rates to keep pace with uplift.

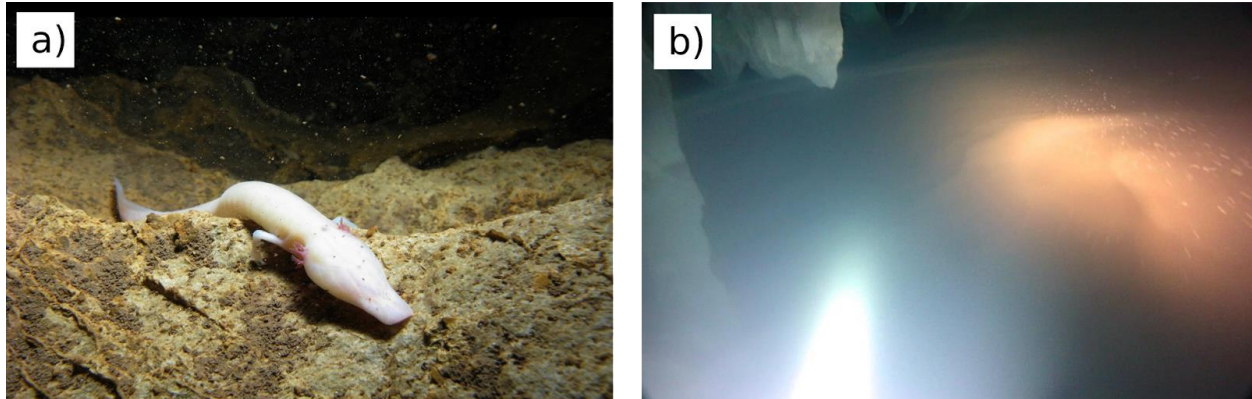
754 The mix of carbonate and non-carbonate minerals within a single rock layer is also an  
755 important control on the roles of chemical and mechanical weathering. When impure carbonates  
756 weather, they leave behind residual material that must be removed from the landscape via  
757 mechanical processes. If the quantity of this material exceeds the transport capacity of the karst  
758 conduit system, then sediment will be routed overland via hillslope and fluvial processes. On the  
759 other hand, chemical weathering of carbonate minerals can dominate weathering fluxes in glacial  
760 landscapes, where physical weathering creates extremely small grain sized sediment, even where  
761 carbonate minerals are only a minor fraction of the bedrock (Scribner et al., 2015; Deuerling et  
762 al., 2019).

763 Chemical and physical processes can also interact in many ways, potentially enhancing or  
764 inhibiting each other. Experiments in subcritical cracking demonstrate unique fracture  
765 propagation behaviors in carbonates, which may relate to dissolution processes at fracture tips  
766 (Atkinson, 1984; Henry, 1978). In general, models and experiments suggest that acids can  
767 enhance fracture propagation rates in carbonate rocks (e.g., Hu & Hueckel, 2019). Roots are an  
768 important agent in mechanical breakup of rock, particularly in areas with thin regolith (Brantley  
769 et al., 2017). In carbonates, roots can take advantage of subsurface porosity generated by  
770 dissolution processes (Estrada-Medina et al., 2013), and they can also generate subsurface  
771 porosity through dissolution by root exudates or CO<sub>2</sub> generated by root respiration (Klappa,  
772 1980; Rossinsky and Wanless, 1992), potentially providing a foothold for root-driven rock  
773 fracturing. It has also been hypothesized that chemical and mechanical erosion may enhance  
774 each other within stream channels (Covington, 2014; Covington & Perne, 2015), with chemical  
775 erosion potentially loosening grains that are then removed by mechanical processes (Emmanuel  
776 & Levenson, 2014), or with mechanical abrasion removing surface impurities to expose fresh  
777 weatherable carbonate minerals. Mechanical weathering processes can also inhibit chemical  
778 weathering processes. For example, buildup of fractured rock material on the surface, with high  
779 surface areas for reaction, may lead to saturation of meteoric water before it reaches unweathered  
780 bedrock. Similarly, high sediment loads within streams could armor the beds and inhibit  
781 dissolution except during periods of sediment mobility.

### 782 3.6 Biota

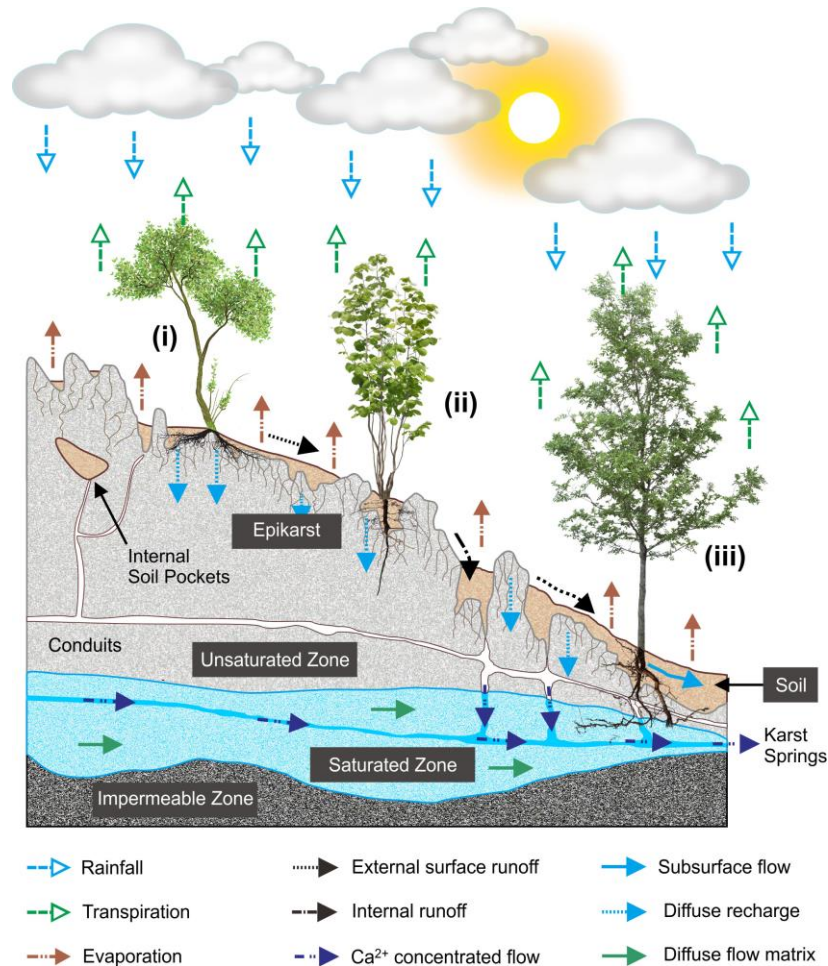
783 As in the CZ more generally, the activity and spatial architecture of carbonate CZ  
784 biological communities have important feedbacks to other CZ processes. Thanks to networks of  
785 large voids, the carbonate CZ is distinguished by the potential for macroscopic biota including  
786 fish, amphibians, and invertebrates to penetrate up to several km below the photic zone (Figure  
787 9). Because both locomotion and passive transport in karst conduit networks are more  
788 constrained than at the surface, carbonate CZ biological communities often show a high degree  
789 of endemism. The resulting small population sizes leave carbonate CZ fauna especially  
790 vulnerable to extinction (Culver & Pipan, 2013).

791 Animal communities in the subsurface can be fed either by in situ microbial primary  
792 production or detrital dissolved and particulate organic carbon percolating downward from the  
793 surface soil. In some cases, sedimentation of particulate organic carbon in conduits creates a  
794 biological hot spot where CO<sub>2</sub> production from decomposition drives further carbonate  
795 dissolution (Covington et al., 2013; Gulley et al., 2016). In coastal karst landscapes where aquifers  
796 are density stratified and partially filled by anoxic seawater (i.e. anchialine), organic matter hot  
797 spots also facilitate H<sub>2</sub>S production from microbial sulfate reduction. As water flows over the hot  
798 spot, H<sub>2</sub>S is transported away and oxidized at redox interfaces elsewhere in the network,  
799 producing sulfuric acid that drives more carbonate dissolution. A striking example of this process  
800 can be observed in the Bahamas eogenetic karst. “Blue holes” (sinkholes) are extremely common  
801 in the landscape and collect surface vegetation, which is deposited at the bottom of the conduit in  
802 anoxic or dysoxic seawater. Tidal pumping exchanges low pH water between the blue hole and  
803 matrix porosity of these eogenetic karst features, enhancing dissolution reactions (Martin et al.,  
804 2012). Decomposition of the detrital plant material fuels intense H<sub>2</sub>S production and, where the  
805 H<sub>2</sub>S diffuses into the photic zone, associated blooms of sulfide-dependent photosynthetic  
806 bacteria thrive and fix additional carbon in the subsurface (Gonzalez et al., 2011, Haas et al.,  
807 2018).



808  
 809 **Figure 9.** a) *Proteus anguinus*, an aquatic salamander found in the karst of the Dinaric Alps that  
 810 is one of the largest cave adapted animals in the world (reaching up to 40 cm in length). Photo  
 811 Gergő Balázs. b) A dense swarm of amphipods (*Niphargus* sp.) flee a diver exploring water-  
 812 filled karst conduits ~400 m below land surface in the Frasassi cave system, Italy. Stable  
 813 density stratification between sulfidic water and an overlying lense of oxic vadose water in the  
 814 aquifer create enough chemical energy to support a rich food web based on microbial  
 815 lithoautotrophy. Photo J. L. Macalady/A. Crocetti.

816 Vegetation on karst landscapes is affected by (1) rapid drainage and associated nutrient  
 817 leaching due to thin soils and large bedrock pores, (2) phosphorous scarcity due to the low P  
 818 content of carbonate bedrock and high phosphate complexation with abundant  $\text{Ca}^{2+}$  ions, (3)  
 819 strong decimeter- to meter-scale spatial heterogeneity in topography, soil and hydrologic factors,  
 820 and (4) slow soil formation due to low availability of silicates to form clay minerals during  
 821 weathering. The plant ecology of tropical and subtropical karst ecosystems has recently been  
 822 reviewed in depth (Geekiyana et al., 2019). Because water in thin karst soils is in short supply,  
 823 plants growing on carbonate-dominated landscapes have adaptations for using alternative  
 824 reservoirs of water, especially in dry seasons (Figure 10). Non-tree species often have  
 825 particularly dense and extensive shallow root systems because they depend on soil water year-  
 826 round (Ellsworth et al., 2015). Due to high bedrock porosity, water stored in the vadose zone  
 827 (epikarst) represents a significant alternative to soil water for woody species that can penetrate  
 828 into carbonate bedrock (e.g., Querejeta et al., 2007). Some woody species also have specialized,  
 829 long roots that reach the water table (Deng et al., 2012; Swaffer et al., 2014). Adaptations for  
 830 obtaining fog water (Fu et al., 2016), and a drought-deciduous strategy in which leaves are shed  
 831 during dry seasons (Reich and Borchert, 1984; Wolfe and Jursar, 2015), have also been  
 832 documented in plants growing in carbonate terrains. Plant adaptations to obtain water resources  
 833 in the carbonate CZ significantly alter the hydrologic balance at depths far below the soil zone,  
 834 and therefore have feedbacks on weathering rates and nutrient and organic carbon transport out  
 835 of the system that are different than in the silicate-dominated CZ (Huang et al., 2009; Dammeyer  
 836 et al., 2016). Karst plant nutrient acquisition strategies may also differ significantly, with  
 837 potential feedback to weathering rates. Plants growing on calcareous soils release organic acids  
 838 from their roots in order to obtain phosphate (Ström et al., 2005). Subsequent microbial  
 839 degradation of the organics further enhances  $\text{CO}_2$  production near roots. In the presence of strong  
 840 topographic heterogeneity leading to soil pockets in epikarst depressions, vegetation can  
 841 reinforce  $\text{CO}_2$ -induced weathering hot spots in the landscape and thereby amplify dissolution  
 842 along certain water flow paths. A well-studied example of spatial patterning due to vegetation-  
 843 mediated positive weathering feedbacks can be seen in Big Cypress National Preserve, South  
 844 Florida (Dong et al., 2019a,b).



845 **Figure 10.** Water use strategies of karst plant species in a typical karst ecosystem during the dry  
 846 season; (i) soil water dependent (species that predominantly take up soil water in both the dry  
 847 and wet season), (ii) epikarst water dependent (species that use both soil and water stored in  
 848 epikarst in both seasons and show a major shift to epikarst water when soil water is depleted  
 849 during the dry season), and (iii) groundwater dependent (species that use groundwater in  
 850 addition to soil and epikarst water and show a major shift to epikarst and groundwater when  
 851 soil water is depleted during the dry season). Not illustrated here are (iv) fog water dependent  
 852 plants, which use fog-derived water in addition to any of the above water sources, and (v)  
 853 drought-deciduous (remain dormant by leaf shedding during the dry season). From  
 854 Geekiyanage et al. (2019).  
 855

856

857 Karst uplands are vulnerable to runaway degradation if trees are removed. In the absence  
 858 of forest vegetation protecting thin soils, rapid erosion into exposed karst fissures culminates in  
 859 the creation of rocky deserts where forest vegetation can no longer get a foothold. Rocky  
 860 desertification has occurred in significant areas of Mediterranean Europe (e.g., the Dinaric  
 861 Karst), on islands such as Haiti and Barbados in the Caribbean, and especially and most recently  
 862 in southwestern China (Jiang et al., 2014; Green et al., 2019). Over the past 50 years, a variety of  
 863 human activities have played a substantial role in the expansion of rocky deserts in China

864 including fuelwood collection, development of housing and tourism, slope cultivation, and  
865 animal grazing (Zhao and Hou, 2019).

## 866 **5 Conclusions**

867 Carbonates underlie a substantial portion of Earth's surface and represent an important  
868 fraction of Earth's CZ, providing crucial water resources and ecosystem services to more than a  
869 billion people. Our current state of knowledge suggests that the congruent weathering, high  
870 solubility, and fast kinetics of carbonate dissolution, lead to altered rates and patterns of CZ  
871 evolution in carbonates compared to silicate settings. When landscapes develop in relatively pure  
872 carbonate rocks, karst systems typically form, producing large contrasts in subsurface  
873 permeability and long-range subsurface connectivity that enable rapid fluxes of water, solutes,  
874 sediment, and gases through the carbonate CZ along routes of preferential flow. Direct  
875 relationships between biological CO<sub>2</sub> production and carbonate weathering by carbonic acid  
876 mean that production of porosity in the subsurface may be tied to biological processes in  
877 carbonates, potentially enabling carbonate-specific feedback loops between CZ development and  
878 ecosystem form and function. Similar feedback occurs with other natural and anthropogenic  
879 acids including sulfuric and nitric acids. Because of the rapid kinetics of calcite dissolution,  
880 shifts in system dynamics and structure due to changes in ecology, land use, or climate may also  
881 be rapid.

882 These differences show that conceptual models developed to understand CZ architecture  
883 and evolution within silicate-rich rocks, such as the conveyor model, may require substantial  
884 rethinking in their application to carbonates. We present the initial ideas of a "dissolving  
885 conveyor" and a "leaky conveyor" as starting points to incorporate carbonate CZ processes. The  
886 ability of karst conduits to transport mobile regolith can lead to decoupling of hillslopes from  
887 stream channels, potentially weakening or eliminating feedback mechanisms that drive  
888 landscapes underlain by silicate-rich rocks toward equilibrium topography and regolith  
889 thickness. The fast reaction kinetics and elevated solubility of carbonate minerals lead to distinct  
890 differences in the relationships between tectonism and carbonate and silicate CZ development,  
891 including interactions between base level and the depths of weathering processes. Because of the  
892 deep circulation of meteoric water in karst settings, the lower boundary of the CZ needs to be  
893 expanded, and the definition of the CZ may need modification to include carbonate terrain.

894 A better understanding of carbonate CZ development may inspire broader conceptual  
895 frameworks that incorporate roles for preferential flow and heterogeneity, which are present to  
896 some extent in all CZ settings. The triple porosity system of matrix, fractures, and karst provides  
897 opportunities to study a spectrum of flow-through timescales and weathering rates and depths in  
898 one setting. Scaling questions are also amplified when there are large contrasts in permeability  
899 that vary with the scale considered. The controlling processes in the conveyor model for  
900 weathering might be better understood by measuring rates in a faster transport system,  
901 particularly under anthropogenic stresses, harking back to the concept of carbonate rocks as a  
902 bellwether. Constraining the transport of gases through the subsurface may enhance our  
903 understanding of the global carbon cycle and how it is affected by biological and geochemical  
904 processes.

905 In any case, understanding how the CZ evolves along the carbonate-silicate spectrum  
906 requires a broader conceptual framework than we currently have. Many questions arise. What  
907 controls the distribution of CO<sub>2</sub> in the subsurface? How do *p*CO<sub>2</sub>, water availability, plant  
908 growth and rock structure interact to determine patterns of porosity development? Under what

909 conditions do acids other than carbonic acid drive porosity development? How are feedbacks  
910 between biological, hydrological, and geological processes reflected at the landscape scale?  
911 There is also a need to integrate knowledge across sites rather than focusing on the idiosyncratic  
912 or distinctive nature of individual sites. In addition to pure carbonates and pure silicates, there is  
913 an entire spectrum of mixtures that lie between these endmembers. What are the most important  
914 parameters along that spectrum that produce differences in CZ processes and architecture?  
915 Answers to these questions will require transdisciplinary study teams that are integrated into the  
916 critical zone research community going forward.

917

918

### 919 **Acknowledgments**

920 This work was supported by the National Science Foundation grant CZ RCN: Research  
921 Coordination Network in Carbonate Critical Zones (1905259). PLS was also supported by CZ  
922 RCN: Expanding Knowledge of Earth's Critical Zone (1904527).

### 923 **Open Research**

924 No new data were presented in this review article.

925

### 926 **References**

927 Adams, P. N., Opdyke, N. D., & Jaeger, J. M. (2010). Isostatic uplift driven by karstification and  
928 sea-level oscillation: Modeling landscape evolution in north Florida. *Geology*, 38(6), 531-534.  
929 <https://doi.org/10.1130/G30592.1>

930 Allred, K. (2004). Some carbonate erosion rates of southeast Alaska. *Journal of Cave and Karst*  
931 *Studies*, 66(3), 89-97.

932 Álvarez Nazario, M. (1972). La herencia lingüística de Canarias en Puerto Rico. *San Juan:*  
933 *Instituto de Cultura Puertorriqueña*, 136-151.

934 Amundson, R., Richter, D. D., Humphreys, G. S., Jobbágy, E. G., & Gaillardet, J. (2007).

935 Coupling between biota and earth materials in the critical zone. *Elements*, 3(5), 327-332.

936 <https://doi.org/10.2113/gselements.3.5.327>

- 937 Anderson, R. S., Anderson, S. P., & Tucker, G. E. (2013). Rock damage and regolith transport  
938 by frost: An example of climate modulation of the geomorphology of the critical zone. *Earth*  
939 *Surface Processes and Landforms*, 38(3), 299-316. <https://doi.org/10.1002/esp.3330>
- 940 Anderson, S. P., Dietrich, W. E., & Brimhall Jr, G. H. (2002). Weathering profiles, mass-balance  
941 analysis, and rates of solute loss: Linkages between weathering and erosion in a small, steep  
942 catchment. *Geological Society of America Bulletin*, 114(9), 1143-1158.  
943 [https://doi.org/10.1130/0016-7606\(2002\)114<1143:WPMBAA>2.0.CO;2](https://doi.org/10.1130/0016-7606(2002)114<1143:WPMBAA>2.0.CO;2)
- 944 Andrews, J. A., & Schlesinger, W. H. (2001). Soil CO<sub>2</sub> dynamics, acidification, and chemical  
945 weathering in a temperate forest with experimental CO<sub>2</sub> enrichment. *Global biogeochemical*  
946 *cycles*, 15(1), 149-162. <https://doi.org/10.1029/2000GB001278>
- 947 Ashton, K. (1966). The analysis of flow data from karst drainage systems. *Transactions of the*  
948 *Cave Research Group of Great Britain*, 7(2), 161–204.
- 949 Atkinson, T. C. (1977a). Diffuse flow and conduit flow in limestone terrain in the Mendip Hills,  
950 Somerset (Great Britain). *Journal of Hydrology*, 35(1-2), 93–110. [https://doi.org/10.1016/0022-](https://doi.org/10.1016/0022-1694(77)90079-8)  
951 [1694\(77\)90079-8](https://doi.org/10.1016/0022-1694(77)90079-8)
- 952 Atkinson, T. C. (1977b). Carbon dioxide in the atmosphere of the unsaturated zone: An  
953 important control of groundwater hardness in limestones. *Journal of Hydrology*, 35(1-2), 111–  
954 123. [https://doi.org/10.1016/0022-1694\(77\)90080-4](https://doi.org/10.1016/0022-1694(77)90080-4)
- 955 Audra, P., Bini, A., Gabrovšek, F., Häuselmann, P., Hobléa, F., Jeannin, P.-Y., Kunaver, J.,  
956 Monbaron, M., Šušteršič, F., Tognini, P., Trimmel, H., Wildberger, A. (2007). Cave and Karst  
957 Evolution in the Alps and Their Relation to Paleoclimate and Paleotopography. *Acta*  
958 *Carsologica*, 36(1), 53-67. <https://doi.org/10.3986/ac.v36i1.208>

- 959 Back, W., Hanshaw, B.B., Herman, J.S., Van Driel, J.N. (1986). Differential dissolution of a  
960 Pleistocene reef in the ground-water mixing zone of coastal Yucatan, Mexico. *Geology*, 14(2),  
961 137–140.
- 962 Beaulieu, E., Y. Godd ris, D. Labat, C. Roelandt, D. Calmels, and J. Gaillardet (2011),  
963 Modeling of water-rock interaction in the Mackenzie basin: Competition between  
964 sulfuric and carbonic acids, *Chemical Geology*, 289(1-2), 114-123.  
965 <https://doi.org/10.1016/j.chemgeo.2011.07.020>
- 966 Beerling, D. J., Woodward, F. I., Lomas, M. R., Wills, M. A., Quick, W. P., & Valdes, P. J.  
967 (1998). The influence of Carboniferous palaeoatmospheres on plant function: an experimental  
968 and modelling assessment. *Philosophical Transactions of the Royal Society of London. Series B:*  
969 *Biological Sciences*, 353(1365), 131-140. <https://doi.org/10.1098/rstb.1998.0196>
- 970 Benavente, J., Vadillo, I., Carrasco, F., Soler, A., Li n n, C., Moral, F. (2010). Air Carbon  
971 Dioxide Contents in the Vadose Zone of a Mediterranean Karst. *Vadose Zone Journal*, 9(1), 126-  
972 136. <https://doi.org/10.2136/vzj2009.0027>
- 973 Berner, R.A. (1992). Weathering, plants, and the long-term carbon cycle. *Geochimica et*  
974 *Cosmochimica Acta*, 56(8), 3225–3231. [https://doi.org/10.1016/0016-7037\(92\)90300-8](https://doi.org/10.1016/0016-7037(92)90300-8)
- 975 Berner, R.A. (1997). The Rise of Plants and Their Effect on Weathering and Atmospheric CO<sub>2</sub>.  
976 *Science*, 276(5312), 544–546. <https://doi.org/10.1126/science.276.5312.544>
- 977 Billings, S. A., Hirmas, D., Sullivan, P. L., Lehmeier, C. A., Bagchi, S., Min, K. et al. (2018).  
978 Loss of deep roots limits biogenic agents of soil development that are only partially restored by  
979 decades of forest regeneration. *Elementa: Science of the Anthropocene*, 6(34).  
980 <https://doi.org/10.1525/elementa.287>
- 981 Birk, S., Liedl, R., & Sauter, M. (2006). Karst Spring Responses Examined by Process-Based  
982 Modeling. *Ground Water*, 44(6), 832–836. <https://doi.org/10.1111/j.1745-6584.2006.00175.x>

- 983 Bögli, A. (1964). Mischungskorrosion — Ein Beitrag zum Verkarstungsproblem. *Erdkunde*, 18,  
984 83–92.
- 985 Brantley, S. L., Eissenstat, D. M., Marshall, J. A., Godsey, S. E., Balogh-Brunstad, Z., Karwan,  
986 D. L., et al. (2017). Reviews and syntheses: on the roles trees play in building and plumbing the  
987 critical zone. *Biogeosciences*, 14(22), 5115-5142.
- 988 Brantley, S.L., Holleran, M.E., Jin, L., & Bazilevskaya, E. (2013). Probing deep weathering in  
989 the Shale Hills Critical Zone Observatory, Pennsylvania (USA): the hypothesis of nested  
990 chemical reaction fronts in the subsurface. *Earth Surf. Process. Landforms*, 38(11), 1280–1298.  
991 <https://doi.org/10.1002/esp.3415>
- 992 Brantley, S.L., Lebedeva, M.I., Balashov, V.N., Singha, K., Sullivan, P.L., & Stinchcomb, G.  
993 (2017a). Toward a conceptual model relating chemical reaction fronts to water flow paths in  
994 hills. *Geomorphology*, 277, 100–117. <https://doi.org/10.1016/j.geomorph.2016.09.027>
- 995 Brantley, S.L., McDowell, W.H., Dietrich, W.E., White, T.S., Kumar, P., Anderson, S.P.,  
996 Chorover, J., Lohse, K.A., Bales, R.C., Richter, D.D., Grant, G., & Gaillardet, J. (2017b).  
997 Designing a network of critical zone observatories to explore the living skin of the terrestrial  
998 Earth. *Earth Surface Dynamics*, 5(4), 841–860. <https://doi.org/10.5194/esurf-5-841-2017>
- 999 Breithaupt, C. I., Gulley, J. D., Bunge, E. M., Moore, P. J., Kerans, C., Fernandez-Ibanez, F., &  
1000 Fullmer, S. M. (2021). A transient, perched aquifer model for banana hole formation: Evidence  
1001 from San Salvador Island, Bahamas. *Earth Surface Processes and Landforms*, 47(2), 618-638.  
1002 <https://doi.org/10.1002/esp.5276>
- 1003 Brookfield, A.E., Macpherson, G.L., & Covington, M.D. (2017). Effects of Changing Meteoric  
1004 Precipitation Patterns on Groundwater Temperature in Karst Environments. *Groundwater*,  
1005 552(2), 227–236. <https://doi.org/10.1111/gwat.12456>

- 1006 Brown, A.L., Martin, J.B., Sreaton, E.J., Ezell, J.E., Spellman, P., & Gulley, J. (2014). Bank  
1007 storage in karst aquifers: The impact of temporary intrusion of river water on carbonate  
1008 dissolution and trace metal mobility. *Chemical Geology*, 385, 56–69.  
1009 <https://doi.org/10.1016/j.chemgeo.2014.06.015>
- 1010 Brown, A.L., Martin, J.B., Kamenov, G.D., Ezell, J.E., Sreaton, E.J., Gulley, J., & Spellman, P.  
1011 (2019). Trace metal cycling in karst aquifers subject to periodic river water intrusion. *Chemical*  
1012 *Geology*, 527, 118773. <https://doi.org/10.1016/j.chemgeo.2018.05.020>
- 1013 Brucker, R.W., Hess, J.W., & White, W.B., 1972. Role of Vertical Shafts in the Movement of  
1014 Ground Water in Carbonate Aquifers. *Groundwater*, 10(6), 5–13. [https://doi.org/10.1111/j.1745-](https://doi.org/10.1111/j.1745-6584.1972.tb02943.x)  
1015 [6584.1972.tb02943.x](https://doi.org/10.1111/j.1745-6584.1972.tb02943.x)
- 1016 Choquette, P. W., & L. E. Pray (1970), Geologic nomenclature and classification of porosity in  
1017 sedimentary carbonates, *American Association of Petroleum Geologists Bulletin*, 54(2), 207-250.  
1018 <https://doi.org/10.1306/5D25C98B-16C1-11D7-8645000102C1865D>
- 1019 Cohen, M. J., Watts, D. L., Heffernan, J. B., & Osborne, T. Z. (2011). Reciprocal biotic control  
1020 on hydrology, nutrient gradients, and landform in the greater everglades. *Critical Reviews in*  
1021 *Environmental Science and Technology*, 41(S1), 395-429.  
1022 <https://doi.org/10.1080/10643389.2010.531224>
- 1023 Condon, L. E., Markovich, K. H., Kelleher, C. A., McDonnell, J. J., Ferguson, G., & McIntosh,  
1024 J. C. (2020). Where is the bottom of a watershed?. *Water Resources Research*, 56(3),  
1025 e2019WR026010. <https://doi.org/10.1029/2019WR026010>.
- 1026 Cooper, M.P., & Covington, M.D. (2020). Modeling cave cross-section evolution including  
1027 sediment transport and paragenesis. *Earth Surface Processes and Landforms*, 45(11), 2588–  
1028 2602. <https://doi.org/10.1002/esp.4915>

- 1029 Covington, M. D. (2014). Calcite dissolution under turbulent flow conditions: a remaining  
1030 conundrum. *Acta Carsologica*, 43(1).
- 1031 Covington, M.D. (2016). The importance of advection for CO<sub>2</sub> dynamics in the karst critical  
1032 zone: An approach from dimensional analysis, in: *Geological Society of America Special Papers*  
1033 *516: Caves and Karst Across Time*, Geological Society of America, pp. 113–127.  
1034 [https://doi.org/10.1130/2015.2516\(09\)](https://doi.org/10.1130/2015.2516(09))
- 1035 Covington, M. D., Knierim, K. J., Young, H. A., Rodriguez, J., & Gnoza, H. G. (2021). The  
1036 impact of ventilation patterns on calcite dissolution rates within karst conduits. *Journal of*  
1037 *Hydrology*, 593, 125824. <https://doi.org/10.1016/j.jhydrol.2020.125824>
- 1038 Covington, M. D., Luhmann, A. J., Wicks, C. M., & Saar, M. O. (2012). Process length scales  
1039 and longitudinal damping in karst conduits. *Journal of Geophysical Research: Earth Surface*,  
1040 117(F1). <https://doi.org/10.1029/2011JF002212>
- 1041 Covington, M. D., & Perne, M. (2015). Consider a cylindrical cave: A physicist's view of cave  
1042 and karst science. *Acta Carsologica*, 44(3).
- 1043 Covington, M.D., Prelovšek, M., & Gabrovšek, F. (2013). Influence of CO<sub>2</sub> dynamics on the  
1044 longitudinal variation of incision rates in soluble bedrock channels: feedback mechanisms,  
1045 *Geomorphology*, 186, 85-95, <https://doi:10.1016/j.geomorph.2012.12.025>.
- 1046 Covington, M.D., Vaughn, K.A. (2019). Carbon dioxide and dissolution rate dynamics within a  
1047 karst underflow-overflow system, Savoy Experimental Watershed, Arkansas, USA. *Chemical*  
1048 *Geology*, 527, 118689. <https://doi.org/10.1016/j.chemgeo.2018.03.009>
- 1049 Culver, D.C., Pipan, T., 2013. Subterranean Ecosystems, in: Levin, S.A. (Ed), *Encyclopedia of*  
1050 *Biodiversity*. Academic Press, pp. 49–62. <https://doi.org/10.1016/B978-0-12-384719-5.00224-0>
- 1051 Cvijić, J. (1924). Types morphologiques des terrains calcaires. *Bulletin of the Serbian*  
1052 *geographical society*, 10(1), 1-7.

- 1053 D'Angeli, I. M., Parise, M., Vattano, M., Madonia, G., Galdenzi, S., & De Waele, J. (2019).  
1054 Sulfuric acid caves of Italy: A review. *Geomorphology*, *333*, 105-122.  
1055 <https://doi.org/10.1016/j.geomorph.2019.02.025>.
- 1056 Dammeyer, H. C., Schwinning, S., Schwartz, B. F., & Moore, G. W. (2016). Effects of juniper  
1057 removal and rainfall variation on tree transpiration in a semi-arid karst: Evidence of complex  
1058 water storage dynamics. *Hydrological Processes*, *30*, 4568–4581.
- 1059 Davis, D.G., 1980. Cave development in the Guadalupe Mountains: a critical review of recent  
1060 hypotheses. *NSS Bulletin*, *42*, 42–48.
- 1061 Davis, D. M., & Engelder, T. (1985). The role of salt in fold-and-thrust belts. *Tectonophysics*,  
1062 *119*(1-4), 67-88.
- 1063 Deng, Y., Jiang, Z., & Qin, X. (2012). Water source partitioning among trees growing on  
1064 carbonate rock in a subtropical region of Guangxi, China. *Environmental Earth Sciences*, *66*,  
1065 635–640.
- 1066 Deuerling, K. M., Martin, J. B., Martin, E. E., Abermann, J., Myreng, S. M., Petersen, D., &  
1067 Rennermalm, Å. K. (2019). Chemical weathering across the western foreland of the Greenland  
1068 Ice Sheet. *Geochimica et Cosmochimica Acta*, *245*, 426-440.
- 1069 Dominguez-Cristobal, C. (1989). *La Toponimia del Ciales decimonónico (Vol. 1)*. Instituto  
1070 Internacional de Dasonomía Tropical, San Juan.
- 1071 Dominguez-Cristobal, C. (1992). *La Toponimia del Ciales decimonónico (Vol. 2)*. Instituto  
1072 Internacional de Dasonomía Tropical, San Juan.
- 1073 Cristóbal, C. M. D. (2007). Leyendas indígenas de la zona del carso norteño de Puerto Rico: el  
1074 caliche de Ciales. *Acta Científica*, *21*(1-3), 81-83.
- 1075 Dong, X., Cohen, M. J., Martin, J. B., McLaughlin, D. L., Murray, A. B., Ward, N. D., et al.  
1076 (2019a). Ecohydrologic processes and soil thickness feedbacks control limestone-weathering

- 1077 rates in a karst landscape. *Chemical Geology*, 527, 118774.  
1078 <https://doi.org/10.1016/j.chemgeo.2018.05.021>
- 1079 Dong, X., Murray, A.B., & Heffernan, J.B. (2019b). Ecohydrologic feedbacks controlling sizes  
1080 of cypress wetlands in a patterned karst landscape. *Earth Surface Processes and Landforms*, 44,  
1081 1178–1191. <https://doi.org/10.1002/esp.4564>
- 1082 Drake, J. J. (1980). The effect of soil activity on the chemistry of carbonate groundwaters. *Water*  
1083 *Resources Research*, 16(2), 381-386. <https://doi.org/10.1029/WR016i002p00381>
- 1084 Drever, J.I. (1994). The effect of land plants on weathering rates of silicate minerals. *Geochimica*  
1085 *et Cosmochimica Acta*, 58, 2325–2332. [https://doi.org/10.1016/0016-7037\(94\)90013-2](https://doi.org/10.1016/0016-7037(94)90013-2)
- 1086 Dreybrodt, W. (1990). The Role of Dissolution Kinetics in the Development of Karst Aquifers in  
1087 Limestone: A Model Simulation of Karst Evolution. *The Journal of Geology*, 98, 639–655.
- 1088 Dreybrodt, W. (1996). Principles of Early Development of Karst Conduits Under Natural and  
1089 Man-Made Conditions Revealed by Mathematical Analysis of Numerical Models. *Water Resour.*  
1090 *Res.*, 32, 2923–2935. <https://doi.org/10.1029/96WR01332>
- 1091 C. Dubois, Y. Quinif, J.-M. Baele, L. Barriquand, A. Bini, L. Bruxelles, G. Dandurand, C.  
1092 Havron, O. Kaufmann, B., Lans, R. Maire, J. Martin, J. Rodet, M.D., et al. (2014). The process  
1093 of ghost-rock karstification and its role in the formation of cave systems, *Earth Sci. Rev.*, 131,  
1094 166-148.
- 1095 Engel, A. S., L. A. Stern, & P. C. Bennett (2004), Microbial contributions to cave formation:  
1096 New insights into sulfuric acid speleogenesis, *Geology*, 32(5), 369-372.
- 1097 Egemeier, S.J. (1987). A theory for the origin of Carlsbad Caverns. *NSS Bulletin*. 49, 73–76.
- 1098 Egemeier, S. J. (1988), Cavern development by thermal water, *NSS Bulletin*, 43, 31-51.

- 1099 Ellsworth, P. Z., & Sternberg, L. S. L. (2015). Seasonal water use by deciduous and evergreen  
1100 woody species in a scrub community is based on water availability and root distribution.  
1101 *Ecohydrology*, 8, 538–551.
- 1102 Estrada-Medina, H., Graham, R. C., Allen, M. F., Jiménez-Osornio, J. J., & Robles-Casolco, S.  
1103 (2013). The importance of limestone bedrock and dissolution karst features on tree root  
1104 distribution in northern Yucatán, México. *Plant and soil*, 362(1), 37-50.
- 1105 Ewers, O.R. (1982). *Cavern development in the dimensions of length and breadth* (Doctoral  
1106 dissertation). Hamilton, Canada: McMaster University.
- 1107 Faimon, J., Lang, M., Geršl, M., Sracek, O., & Bábek, O. (2020). The “breathing spots” in karst  
1108 areas—the sites of advective exchange of gases between soils and adjacent underground cavities.  
1109 *Theoretical and Applied Climatology*, 142(1), 85-101. [https://doi.org/10.1007/s00704-020-](https://doi.org/10.1007/s00704-020-03280-7)  
1110 03280-7
- 1111 Fairchild, I. J., Smith, C. L., Baker, A., Fuller, L., Spötl, C., Matthey, D., & McDermott, F.  
1112 (2006). Modification and preservation of environmental signals in speleothems. *Earth-Science*  
1113 *Reviews*, 75(1-4), 105-153. <https://doi.org/10.1016/j.earscirev.2005.08.003>
- 1114 Farrant, A.R., & Smart, P.L. (2011). Role of sediment in speleogenesis; sedimentation and  
1115 paragenesis. *Geomorphology*, 134, 79–93. <https://doi.org/10.1016/j.geomorph.2011.06.006>
- 1116 Filipponi, M., Jeannin, P.-Y., & Tacher, L. (2009). Evidence of inception horizons in karst  
1117 conduit networks. *Geomorphology*, 106, 86–99. <https://doi.org/10.1016/j.geomorph.2008.09.010>
- 1118 Fishedick, M., Roy, J., Acquaye, A., Allwood, J., Ceron, J. P., Geng, Y., et al. (2014). Industry  
1119 In: *Climate Change 2014: Mitigation of Climate Change. Contribution of Working Group III to*  
1120 *the Fifth Assessment Report of the Intergovernmental Panel on Climate Change*. Technical  
1121 Report. Cambridge University Press, Cambridge, United Kingdom.

- 1122 Flint, M. K., Martin, J. B., Summerall, T. I., Barry-Sosa, A., & Christner, B. C. (2021). Nitrous  
1123 oxide processing in carbonate karst aquifers. *Journal of hydrology*, 594, 125936.
- 1124 Florea, L.J., & Vacher, H.L. (2006). Springflow Hydrographs: Eogenetic vs. Telogenetic Karst.  
1125 *Ground Water*, 44, 352–361. <https://doi.org/10.1111/j.1745-6584.2005.00158.x>
- 1126 Florea, L.J., Vacher, H.L., Donahue, B., & Naar, D. (2007). Quaternary cave levels in peninsular  
1127 Florida. *Quaternary Science Reviews*, 26, 1344–1361.  
1128 <https://doi.org/10.1016/j.quascirev.2007.02.011>
- 1129 Fohlmeister, J., Voarintsoa, N.R.G., Lechleitner, F.A., Boyd, M., Brandtstätter, S., Jacobson,  
1130 M.J., & Oster, J.L. (2020). Main controls on the stable carbon isotope composition of  
1131 speleothems. *Geochimica et Cosmochimica Acta*, 279, 67–87.  
1132 <https://doi.org/10.1016/j.gca.2020.03.042>
- 1133 Ford, D. C. (1971). Alpine Karst in the Mt. Castleguard-Columbia icefield area, Canadian Rocky  
1134 Mountains. *Arctic and Alpine Research*, 3(3), 239-252.
- 1135 Ford, D. C., Lauritzen, S. E., & Ewers, R. O. (2000). Modeling of initiation and propagation of  
1136 single conduits and networks. *Speleogenesis: Evolution of Karst Aquifers*. Huntsville, Ala.,  
1137 *National Speleological Society*, 175-183.
- 1138 Ford, D., & Williams, P.D. (2007). *Karst hydrogeology and geomorphology*. John Wiley &  
1139 Sons.
- 1140 Frumkin, A., 2013. Salt karst. In: Shroder, J. (Editor in Chief), Frumkin, A. (Ed.), *Treatise on*  
1141 *Geomorphology, Karst Geomorphology*. Academic Press, San Diego, CA, 407-424.
- 1142 Fu, T., Chen, H., Fu, Z., & Wang, K. (2016). Surface soil water content and its controlling  
1143 factors in a small karst catchment. *Environmental Earth Sciences*, 75, 1406.
- 1144 Gabrovšek, F. (2009). On concepts and methods for the estimation of dissolutional denudation  
1145 rates in karst areas. *Geomorphology*, 106, 9–14. <https://doi.org/10.1016/j.geomorph.2008.09.008>

- 1146 Gabrovšek, F., & Dreybrodt, W. (2001). A model of the early evolution of karst aquifers in  
1147 limestone in the dimensions of length and depth. *Journal of Hydrology*, *240*, 206–224.  
1148 [https://doi.org/10.1016/S0022-1694\(00\)00323-1](https://doi.org/10.1016/S0022-1694(00)00323-1)
- 1149 Gabrovšek, F., Häuselmann, P., & Audra, P. (2014). ‘Looping caves’ versus ‘water table caves’:  
1150 The role of base-level changes and recharge variations in cave development. *Geomorphology*,  
1151 *204*, 683–691. <https://doi.org/10.1016/j.geomorph.2013.09.016>
- 1152 Gaillardet, J., Calmels, D., Romero-Mujalli, G., Zakharova, E., & Hartmann, J. (2019). Global  
1153 climate control on carbonate weathering intensity. *Chemical Geology*, *527*, 118762.  
1154 <https://doi.org/10.1016/j.chemgeo.2018.05.009>
- 1155 Galloway, J. N. (1998). The global nitrogen cycle: changes and consequences. *Environmental*  
1156 *pollution*, *102*(1), 15-24.
- 1157 Galloway, J. N., Townsend, A. R., Erisman, J. W., Bekunda, M., Cai, Z., Freney, J. R., et al.  
1158 (2008). Transformation of the nitrogen cycle: recent trends, questions, and potential solutions.  
1159 *Science*, *320*(5878), 889-892.
- 1160 Gandois, L., A.-S. Perrin, & A. Probst (2011). Impact of nitrogenous fertiliser-induced proton  
1161 release on cultivated soils with contrasting carbonate contents: a column experiment.  
1162 *Geochimica et cosmochimica acta*, *75*(5): 1185-1198.
- 1163 Garcia, A. A., Semken, S., & Brandt, E. (2020). The Construction of Cultural Consensus Models  
1164 to Characterize Ethnogeological Knowledge. *Geoheritage*, *12*(3), 59.  
1165 <https://doi.org/10.1007/s12371-020-00480-5>
- 1166 Geekiyanage, N., Goodale, U. M., Cao, K., & Kitajima, K. (2019). Plant ecology of tropical and  
1167 subtropical karst ecosystems. *Biotropica*, *51*(5), 626-640.

- 1168 Goldscheider, N., Chen, Z., Auler, A. S., Bakalowicz, M., Broda, S., Drew, D., et al. (2020).  
1169 Global distribution of carbonate rocks and karst water resources. *Hydrogeology Journal*, 28(5),  
1170 1661-1677. <https://doi.org/10.1007/s10040-020-02139-5>
- 1171 Gombert, P. (2002). Role of karstic dissolution in global carbon cycle. *Global and Planetary*  
1172 *Change*, 33, 177–184. [https://doi.org/10.1016/S0921-8181\(02\)00069-3](https://doi.org/10.1016/S0921-8181(02)00069-3)
- 1173 Gonzalez, B. C., Iliffe, T. M., Macalady, J. L., Schaperdoth, I., & Kakuk, B. (2011). Microbial  
1174 hotspots in anchialine blue holes: initial discoveries from the Bahamas. *Hydrobiologia*, 677(1),  
1175 149-156.
- 1176 Granger, D.E., Fabel, D., & Palmer, A.N. (2001). Pliocene-Pleistocene incision of the Green  
1177 River, Kentucky, determined from radioactive decay of cosmogenic <sup>26</sup>Al and <sup>10</sup>Be in Mammoth  
1178 Cave sediments. *Geological Society of America Bulletin*, 113, 825–836.
- 1179 Green, S.M., Dungait, J.A.J., Tu, C., Buss, H.L., Sanderson, N., Hawkes, S.J., et al. (2019). Soil  
1180 functions and ecosystem services research in the Chinese karst Critical Zone. *Chemical Geology*,  
1181 527, 119107. <https://doi.org/10.1016/j.chemgeo.2019.03.018>
- 1182 Groves, C., & Hendrikson, M. (2011). From sink to resurgence: the buffering capacity of a cave  
1183 system in the Tongass National Forest, USA. *Acta Carsologica*, 391.
- 1184 Groves, C.G., & Howard, A.D. (1994). Minimum hydrochemical conditions allowing limestone  
1185 cave development. *Water Resour. Res.*, 30, 607–615. <https://doi.org/10.1029/93WR02945>
- 1186 Groves, C., & Meiman, J. (2005). Weathering, geomorphic work, and karst landscape evolution  
1187 in the Cave City groundwater basin, Mammoth Cave, Kentucky. *Geomorphology*, 67, 115–126.  
1188 <https://doi.org/10.1016/j.geomorph.2004.07.008>
- 1189 Gulley, J.D., Martin, J.B., & Brown, A. (2016). Organic carbon inputs, common ions and  
1190 degassing: rethinking mixing dissolution in coastal eogenetic carbonate aquifers: Rethinking

- 1191 Mixing Dissolution in Coastal Eogenetic Carbonate Aquifers. *Earth Surf. Process. Landforms*,  
1192 *41*, 2098–2110. <https://doi.org/10.1002/esp.3975>
- 1193 Gulley, J.D., Martin, J.B., Moore, P.J., Brown, A., Spellman, P.D., & Ezell, J. (2015).  
1194 Heterogeneous distributions of CO<sub>2</sub> may be more important for dissolution and karstification in  
1195 coastal eogenetic limestone than mixing dissolution. *Earth Surf. Process. Landforms*, *40*, 1057–  
1196 1071. <https://doi.org/10.1002/esp.3705>
- 1197 Gulley, J.D., Martin, J.B., Moore, P.J., & Murphy, J. (2013). Formation of phreatic caves in an  
1198 eogenetic karst aquifer by CO<sub>2</sub> enrichment at lower water tables and subsequent flooding by sea  
1199 level rise. *Earth Surf. Process. Landforms*, *38*, 1210–1224. <https://doi.org/10.1002/esp.3358>
- 1200 Gulley, J., Martin, J., & Moore, P. (2014). Vadose CO<sub>2</sub> gas drives dissolution at water tables in  
1201 eogenetic karst aquifers more than mixing dissolution. *Earth Surf. Process. Landforms*, *39*,  
1202 1833–1846. <https://doi.org/10.1002/esp.3571>
- 1203 Gulley, J., Martin, J.B., Sreaton, E.J., & Moore, P.J. (2011). River reversals into karst springs:  
1204 A model for cave enlargement in eogenetic karst aquifers. *Geological Society of America*  
1205 *Bulletin*, *123*, 457–467. <https://doi.org/10.1130/B30254.1>
- 1206 Gulley, J., Martin, J., Spellman, P., Moore, P., & Sreaton, E. (2013). Dissolution in a variably  
1207 confined carbonate platform: effects of allogenic runoff, hydraulic damming of groundwater  
1208 inputs, and surface-groundwater exchange at the basin scale. *Earth Surf. Process. Landforms*, *38*,  
1209 1700–1713. <https://doi.org/10.1002/esp.3411>
- 1210 Haas, S., De Beer, D., Klatt, J. M., Fink, A., Rench, R. M., Hamilton, T. L., et al. (2018). Low-  
1211 light anoxygenic photosynthesis and Fe-S-biogeochemistry in a microbial mat. *Frontiers in*  
1212 *Microbiology*, *9*, 858.

- 1213 Halihan, T., Sharp, J. M., & Mace, R. E. (2000). Flow in the San Antonio segment of the  
1214 Edwards aquifer: matrix, fractures, or conduits?. In Sasowsky, I. D., & Wicks, C. M. (Eds),  
1215 *Groundwater flow and contaminant transport in carbonate aquifers*. CRC Press. (pp. 129-146).
- 1216 Hanna, R. B., & Rajaram, H. (1998). Influence of aperture variability on dissolutional growth of  
1217 fissures in karst formations. *Water Resources Research*, 34(11), 2843-2853.  
1218 <https://doi.org/10.1029/98WR01528>
- 1219 Hartmann, J., & Moosdorf, N. (2012). The new global lithological map database GLiM: A  
1220 representation of rock properties at the Earth surface. *Geochemistry, Geophysics, Geosystems*,  
1221 13. <https://doi.org/10.1029/2012GC004370>
- 1222 Häuselmann, P., & Tognini, P. (2005). Kaltbach cave (Siebenhengste, Switzerland): Phantom of  
1223 the sandstone? *Acta carsologica*, 34.
- 1224 Heimsath, A.M., Chadwick, O.A., Roering, J.J., & Levick, S.R. (2020). Quantifying erosional  
1225 equilibrium across a slowly eroding, soil mantled landscape. *Earth Surface Processes and*  
1226 *Landforms*, 45, 499–510. <https://doi.org/10.1002/esp.4725>
- 1227 Heimsath, A.M., Dietrich, W.E., Nishiizumi, K., & Finkel, R.C. (1997). The soil production  
1228 function and landscape equilibrium. *Nature*, 388, 358–361. <https://doi.org/10.1038/41056>
- 1229 Henry, P. J. (1978). *Mechanique lineaire de la rupture applique a l'etude de la fissuration et de*  
1230 *la fracture de roches calcaires*, (Doctoral dissertation). Lille, France: Lille University of Science  
1231 and Technology.
- 1232 Herman, E.K., Toran, L., & White, W.B. (2012). Clastic sediment transport and storage in  
1233 fluviokarst aquifers: an essential component of karst hydrogeology. *Carbonates Evaporites*, 27,  
1234 211–241. <https://doi.org/10.1007/s13146-012-0112-7>

- 1235 Hill, C.A. (1990). Sulfuric Acid Speleogenesis of Carlsbad Cavern and Its Relationship to  
1236 Hydrocarbons, Delaware Basin, New Mexico and Texas. *AAPG Bulletin*, 74, 1685–1694.  
1237 <https://doi.org/10.1306/0C9B2565-1710-11D7-8645000102C1865D>
- 1238 Hilley, G.E., Chamberlain, C.P., Moon, S., Porder, S., & Willett, S.D. (2010). Competition  
1239 between erosion and reaction kinetics in controlling silicate-weathering rates. *Earth and*  
1240 *Planetary Science Letters*, 293, 191–199. <https://doi.org/10.1016/j.epsl.2010.01.008>
- 1241 Houillon, N., Lastennet, R., Denis, A., Malaurent, P., Minvielle, S., & Peyraube, N. (2017).  
1242 Assessing cave internal aerology in understanding carbon dioxide (CO<sub>2</sub>) dynamics: implications  
1243 on calcite mass variation on the wall of Lascaux Cave (France). *Environ Earth Sci*, 76, 170.  
1244 <https://doi.org/10.1007/s12665-017-6498-8>
- 1245 Hu, M., & Hueckel, T. (2019). Modeling of subcritical cracking in acidized carbonate rocks via  
1246 coupled chemo-elasticity. *Geomechanics for Energy and the Environment*, 19, 100114.
- 1247 Huang, Y., Zhao, P., Zhang, Z., Li, X., He, C., & Zhang, R. (2009). Transpiration of  
1248 *Cyclobalanopsis glauca* (syn. *Quercus glauca*) stand measured by sap-flow method in a karst  
1249 rocky terrain during dry season. *Ecological Research*, 24, 791–801.
- 1250 Irwin, J. G., & Williams, M. L. (1988). Acid rain: chemistry and transport. *Environmental*  
1251 *Pollution*, 50(1-2), 29-59.
- 1252 Jackson, R.B., Canadell, J., Ehleringer, J.R., Mooney, H.A., Sala, O.E., & Schulze, E.D. (1996).  
1253 A global analysis of root distributions for terrestrial biomes. *Oecologia*, 108, 389–411.  
1254 <https://doi.org/10.1007/BF00333714>
- 1255 Jagnow, D.H., Hill, C.A., Davis, D.G., DuChene, H.R., Cunningham, K.I., Northup, D.E. et al.  
1256 (2000). History of the sulfuric acid theory of speleogenesis in the Guadalupe Mountains, New  
1257 Mexico. *Journal of Cave and Karst Studies*, 62, 54–59.

- 1258 Jiang, Z., Lian, Y., & Qin, X. (2014). Rocky desertification in Southwest China: impacts, causes,  
1259 and restoration. *Earth-Science Reviews*, *132*, 1-12.  
1260 <https://doi.org/10.1016/j.earscirev.2014.01.005>.
- 1261 Jobbágy, E.G., & Jackson, R.B. (2000). The Vertical Distribution of Soil Organic Carbon and Its  
1262 Relation to Climate and Vegetation. *Ecological Applications*, *10*, 423–436.  
1263 [https://doi.org/10.1890/1051-0761\(2000\)010\[0423:TVDOSO\]2.0.CO;2](https://doi.org/10.1890/1051-0761(2000)010[0423:TVDOSO]2.0.CO;2)
- 1264 Jones, D. S., Polerecky, L., Galdenzi, S., Dempsey, B. A. & Macalady, J. L. (2015). Fate of  
1265 sulfide in the Frasassi cave system and implications for sulfuric acid speleogenesis. *Chemical*  
1266 *Geology*, *410*, 21–27.
- 1267 Khadka, M.B., Martin, J.B., & Jin, J. (2014). Transport of dissolved carbon and CO<sub>2</sub> degassing  
1268 from a river system in a mixed silicate and carbonate catchment. *Journal of Hydrology*, *513*,  
1269 391–402.
- 1270 Kim, H., Stinchcomb, G., & Brantley, S.L. (2017). Feedbacks among O<sub>2</sub> and CO<sub>2</sub> in deep soil  
1271 gas, oxidation of ferrous minerals, and fractures: A hypothesis for steady-state regolith thickness.  
1272 *Earth and Planetary Science Letters*, *460*, 29–40. <https://doi.org/10.1016/j.epsl.2016.12.003>
- 1273 Király, L. (1975). Rapport sur l'état actuel des connaissances dans le domaine des caractères  
1274 physiques des roches karstiques. *Hydrogeology of karstic terrains (Hydrogéologie des terrains*  
1275 *karstiques) International Union of geological sciences*, *3*, 53–67.
- 1276 Klappa, C. F. (1980). Brecciation textures and tepee structures in Quaternary calcrete (caliche)  
1277 profiles from eastern Spain: the plant factor in their formation. *Geological Journal*, *15*(2), 81-89.
- 1278 Klimchouk, A. (2004). Towards defining, delimiting and classifying epikarst: Its origin,  
1279 processes and variants of geomorphic evolution. *Speleogenesis and Evolution of Karst Aquifers*,  
1280 *2*, 1–13.
- 1281 Klimchouk, A. B. (2007). Hypogene speleogenesis: Hydrogeological and Morphogenetic  
1282 Perspective. NCKRI-Special Paper 1.

- 1283 Klimchouk, A. (2019). Krubera (Voronja) Cave, in: Encyclopedia of Caves. Elsevier, pp. 627–  
1284 634.
- 1285 Klimchouk, A., Forti, P., & Cooper, A. (1996). Gypsum karst of the World: a brief overview.  
1286 *International Journal of Speleology*, 25, 3-4, 159-181.
- 1287 Kogovšek, J., & Petrič, M. (2012). Characterization of the vadose flow and its influence on the  
1288 functioning of karst springs: Case study of the karst system near Postojna, Slovenia. *Acta*  
1289 *carsologica*, 41.
- 1290 Kowalczyk, A.J., & Froelich, P.N. (2010). Cave air ventilation and CO<sub>2</sub> outgassing by radon-222  
1291 modeling: How fast do caves breathe? *Earth and Planetary Science Letters*, 289, 209–219.  
1292 <https://doi.org/10.1016/j.epsl.2009.11.010>
- 1293 Kůrková, I., Bruthans, J., Balák, F., Slavík, M., Schweigstillová, J., Bruthansová, J., et al. (2019).  
1294 Factors controlling evolution of karst conduits in sandy limestone and calcareous sandstone  
1295 (Turnov area, Czech Republic). *Journal of Hydrology*, 574, 1062–1073.  
1296 <https://doi.org/10.1016/j.jhydrol.2019.05.013>
- 1297 Lang, M., Faimon, J., Godissart, J., & Ek, C. (2017). Carbon dioxide seasonality in dynamically  
1298 ventilated caves: the role of advective fluxes. *Theor Appl Climatol*, 129, 1355–1372.  
1299 <https://doi.org/10.1007/s00704-016-1858-y>
- 1300 Larson, E.B., & Mylroie, J.E. (2018). Diffuse Versus Conduit Flow in Coastal Karst Aquifers:  
1301 The Consequences of Island Area and Perimeter Relationships. *Geosciences*, 8, 268.  
1302 <https://doi.org/10.3390/geosciences8070268>
- 1303 Lebedeva, M.I., Fletcher, R.C., Brantley, S.L. (2010). A mathematical model for steady-state  
1304 regolith production at constant erosion rate. *Earth Surf. Process. Landforms*, 35, 508–524.  
1305 <https://doi.org/10.1002/esp.1954>

- 1306 Lehmann, H. (1936). *Morphologische Studien auf Java: Geog. Abhandlungen, III*, Stuttgart  
1307 1954, 144.
- 1308 Liu, Z., Groves, C., Yuan, D., Meiman, J., Jiang, G., He, S., et al. (2004). Hydrochemical  
1309 variations during flood pulses in the south-west China peak cluster karst: impacts of CaCO<sub>3</sub>–  
1310 H<sub>2</sub>O–CO<sub>2</sub> interactions. *Hydrol. Process.*, *18*, 2423–2437. <https://doi.org/10.1002/hyp.1472>
- 1311 Liu, Z., Li, Q., Sun, H., & Wang, J. (2007). Seasonal, diurnal and storm-scale hydrochemical  
1312 variations of typical epikarst springs in subtropical karst areas of SW China: Soil CO<sub>2</sub> and  
1313 dilution effects. *Journal of Hydrology*, *337*, 207–223.  
1314 <https://doi.org/10.1016/j.jhydrol.2007.01.034>
- 1315 Lowe, D.J., & Gunn, J. (1997). Carbonate speleogenesis: An inception horizon hypothesis. *Acta*  
1316 *Carsologica*, *38*, 457–488.
- 1317 Lucha, P., Gutiérrez, F., Galve, J. P., & Guerrero, J. (2012). Geomorphic and stratigraphic  
1318 evidence of incision-induced halokinetic uplift and dissolution subsidence in transverse  
1319 drainages crossing the evaporite-cored Barbastro–Balaguer Anticline (Ebro Basin, NE Spain).  
1320 *Geomorphology*, *171*, 154–172. <https://doi.org/10.1016/j.geomorph.2012.05.015>.
- 1321 Macpherson, G.L., & Sullivan, P.L. (2019a). Watershed-scale chemical weathering in a  
1322 merokarst terrain, northeastern Kansas, USA. *Chemical Geology*, *527*, 118988.  
1323 <https://doi.org/10.1016/j.chemgeo.2018.12.001>
- 1324 Macpherson, G.L., & Sullivan, P.L. (2019b). Dust, impure calcite, and phytoliths: Modeled  
1325 alternative sources of chemical weathering solutes in shallow groundwater. *Chemical Geology*,  
1326 *527*, 118871. <https://doi.org/10.1016/j.chemgeo.2018.08.007>
- 1327 Martin, J.B. (2017). Carbonate minerals in the global carbon cycle. *Chemical Geology*, *449*, 58–  
1328 72. <https://doi.org/10.1016/j.chemgeo.2016.11.029>

- 1329 Martin, J.B., & Dean, R.W. (1999). Temperature as a natural tracer of short residence times for  
1330 groundwater in karst aquifers. *Karst Modeling. Karst Waters Institute Special Publication, 5*,  
1331 236–242.
- 1332 Martin, J.B., & Dean, R.W. (2001). Exchange of water between conduits and matrix in the  
1333 Floridan aquifer. *Chemical Geology, 179*, 145–165. <https://doi.org/10.1016/S0009->  
1334 [2541\(01\)00320-5](https://doi.org/10.1016/S0009-2541(01)00320-5)
- 1335 Martin, J. B., Gulley, J., & Spellman, P. (2012). Tidal pumping of water between Bahamian blue  
1336 holes, aquifers, and the ocean. *Journal of Hydrology, 416*, 28-38.
- 1337 Martin, J. B., deGrammont, P. C., Covington, M. D., & Toran, L. (2021). A new focus on the  
1338 neglected carbonate critical zone. *EOS, 102*.
- 1339 Matthey, D.P., Atkinson, T.C., Barker, J.A., Fisher, R., Latin, J.-P., Durrell, R., et al. (2016).  
1340 Carbon dioxide, ground air and carbon cycling in Gibraltar karst. *Geochimica et Cosmochimica*  
1341 *Acta, 184*, 88–113. <https://doi.org/10.1016/j.gca.2016.01.041>
- 1342 Milanolo, S., & Gabrovšek, F. (2009). Analysis of Carbon Dioxide Variations in the Atmosphere  
1343 of Srednja Bijambarska Cave, Bosnia and Herzegovina. *Boundary-Layer Meteorol, 131*, 479–  
1344 493. <https://doi.org/10.1007/s10546-009-9375-5>
- 1345 Miorandi, R., Borsato, A., Frisia, S., Fairchild, I.J., & Richter, D.K. (2010). Epikarst hydrology  
1346 and implications for stalagmite capture of climate changes at Grotta di Ernesto (NE Italy): results  
1347 from long-term monitoring. *Hydrol. Process., 24*, 3101–3114. <https://doi.org/10.1002/hyp.7744>
- 1348 Monroe, W.H. (1976). The karst landforms of Puerto Rico (No. 899). US Geological Survey.
- 1349 Moore, O.W., Buss, H.L., Green, S.M., Liu, M., & Song, Z. (2017). The importance of non-  
1350 carbonate mineral weathering as a soil formation mechanism within a karst weathering profile in  
1351 the SPECTRA Critical Zone Observatory, Guizhou Province, China. *Acta Geochim, 36*, 566–  
1352 571. <https://doi.org/10.1007/s11631-017-0237-4>

- 1353 Musgrove, M., & Banner, J.L. (2004). Controls on the spatial and temporal variability of vadose  
1354 dripwater geochemistry: Edwards aquifer, central Texas, *Geochimica et Cosmochimica Acta*, 68,  
1355 1007–1020. <https://doi.org/10.1016/j.gca.2003.08.014>
- 1356 Mylroie, J.E., & Carew, J.L. (1990). The flank margin model for dissolution cave development  
1357 in carbonate platforms. *Earth Surface Processes and Landforms*, 15, 413–424.
- 1358 National Research Council (2001). *Basic research opportunities in earth science*. National  
1359 Academies Press.
- 1360 Opdyke, N. D., Spangler, D. P., Smith, D. L., Jones, D. S., & Lindquist, R. C. (1984). Origin of  
1361 the epeirogenic uplift of Pliocene-Pleistocene beach ridges in Florida and development of the  
1362 Florida karst. *Geology*, 12(4), 226-228.
- 1363 Ott, R. F., Gallen, S. F., Caves Rugenstein, J. K., Ivy-Ochs, S., Helman, D., Fassoulas, C., et al.  
1364 (2019). Chemical versus mechanical denudation in meta-clastic and carbonate bedrock  
1365 catchments on Crete, Greece, and mechanisms for steep and high carbonate topography. *Journal*  
1366 *of Geophysical Research: Earth Surface*, 124(12), 2943-2961.
- 1367 Ott, R. F. (2020). How lithology impacts global topography, vegetation, and animal biodiversity:  
1368 A global-scale analysis of mountainous regions. *Geophysical Research Letters*, 47(20),  
1369 e2020GL088649.
- 1370 Palmer, A.N. (1991). Origin and morphology of limestone caves. *GSA Bulletin*, 103, 1–21.  
1371 [https://doi.org/10.1130/0016-7606\(1991\)103<0001:OAMOLC>2.3.CO;2](https://doi.org/10.1130/0016-7606(1991)103<0001:OAMOLC>2.3.CO;2)
- 1372 Palmer, A.N. (2001). Dynamics of cave development by allogenic water. *Acta carsologica*, 30,  
1373 13–32.
- 1374 Pané, F. R. (1999). *An Account of the Antiquities of the Indians: A New Edition, with an*  
1375 *Introductory Study, Notes, and Appendices by José Juan Arrom*. Duke University Press.

- 1376 Patton, N.R., Lohse, K.A., Godsey, S.E., Crosby, B.T., & Seyfried, M.S. (2018). Predicting soil  
1377 thickness on soil mantled hillslopes. *Nature Communications*, 9, 3329.  
1378 <https://doi.org/10.1038/s41467-018-05743-y>
- 1379 Perrin, A. S., Probst, A., & Probst, J. L. (2008). Impact of nitrogenous fertilizers on carbonate  
1380 dissolution in small agricultural catchments: Implications for weathering CO<sub>2</sub> uptake at regional  
1381 and global scales. *Geochimica et Cosmochimica Acta*, 72(13), 3105-3123.
- 1382 Peterson, E.W., Wicks, C.M., 2005. Fluid and solute transport from a conduit to the matrix in a  
1383 carbonate aquifer system. *Mathematical Geology*, 37, 851-867,
- 1384 Phillips, J.D., Pawlik, Ł., & Šamonil, P. (2019). Weathering fronts. *Earth-Science Reviews*, 198,  
1385 102925. <https://doi.org/10.1016/j.earscirev.2019.102925>
- 1386 Plummer, L.N. (1975). Mixing of sea water with calcium carbonate ground water. *Geological*  
1387 *Society of America Memoir*, 142, 219–236.
- 1388 Plummer, L. N., Wigley, T. M. L., & Parkhurst, D. L. (1978). The kinetics of calcite dissolution  
1389 in CO<sub>2</sub>-water systems at 5 degrees to 60 degrees C and 0.0 to 1.0 atm CO<sub>2</sub>. *American journal of*  
1390 *science*, 278(2), 179-216. <https://doi.org/10.2475/ajs.278.2.179>
- 1391 Plummer, L.N., Parkhurst, D.L., & Wigley, T.M.L. (1979). Critical review of the kinetics of  
1392 calcite dissolution and precipitation. In *Chemical Modeling in Aqueous Systems*. ACS  
1393 Publications, 537-573.
- 1394 Querejeta, J. I., Estrada-Medina, H., Allen, M. F., & Jiménez-Osornio, J. J. (2007). Water source  
1395 partitioning among trees growing on shallow karst soils in a seasonally dry tropical climate.  
1396 *Oecologia*, 152, 26–36.
- 1397 Quinlan, J. F., Davies, G. J., Jones, S. W., & Huntoon, P. W. (1996). The applicability of  
1398 numerical models to adequately characterize ground-water flow in karstic and other triple-

- 1399 porosity aquifers. *Subsurface fluid-flow (ground-water and vadose zone) modeling, ASTM STP,*  
1400 *1288*, 114-133.
- 1401 Reich, P. B., & Borchert, R. (1984). Water stress and tree phenology in a tropical dry forest in  
1402 the lowlands of Costa Rica. *Journal of Ecology*, *72*, 61-74.
- 1403 Rempe, D.M., & Dietrich, W.E. (2014). A bottom-up control on fresh-bedrock topography under  
1404 landscapes. *Proceedings of the National Academy of Sciences*, *111*, 6576–6581.  
1405 <https://doi.org/10.1073/pnas.1404763111>
- 1406 Riebe, C.S., Hahm, W.J., & Brantley, S.L. (2017). Controls on deep critical zone architecture: a  
1407 historical review and four testable hypotheses. *Earth Surface Processes and Landforms*, *42*, 128–  
1408 156. <https://doi.org/10.1002/esp.4052>
- 1409 Romero-Mujalli, G., Hartmann, J., Börker, J., Gaillardet, J., & Calmels, D. (2019). Ecosystem  
1410 controlled soil-rock pCO<sub>2</sub> and carbonate weathering – Constraints by temperature and soil water  
1411 content. *Chemical Geology*, *527*, 118634. <https://doi.org/10.1016/j.chemgeo.2018.01.030>
- 1412 Rossinsky, V., & Wanless, H. R. (1992). Topographic and vegetative controls on calcrete  
1413 formation, Turks and Caicos Islands, British West Indies. *Journal of Sedimentary Research*,  
1414 *62*(1), 84-98.
- 1415 Ryb, U., Matmon, A., Erel, Y., Haviv, I., Katz, A., Starinsky, A., et al. (2014). Controls on  
1416 denudation rates in tectonically stable Mediterranean carbonate terrain. *Geological Society of*  
1417 *America Bulletin*, *126*, 553–568. <https://doi.org/10.1130/B30886.1>
- 1418 Sanchez-Cañete, E. P., Serrano-Ortiz, P., Kowalski, A. S., Oyonarte, C., & Domingo, F. (2011).  
1419 Subterranean CO<sub>2</sub> ventilation and its role in the net ecosystem carbon balance of a karstic  
1420 shrubland. *Geophysical research letters*, *38*(9). <https://doi.org/10.1029/2011GL047077>

- 1421 Scribner, C. A., Martin, E. E., Martin, J. B., Deuerling, K. M., Collazo, D. F., & Marshall, A. T.  
1422 (2015). Exposure age and climate controls on weathering in deglaciated watersheds of western  
1423 Greenland. *Geochimica et Cosmochimica Acta*, *170*, 157-172.
- 1424 Shaughnessy, A. R., Gu, X., Wen, T., & Brantley, S. L. (2021). Machine learning deciphers  
1425 CO<sub>2</sub> sequestration and subsurface flowpaths from stream chemistry. *Hydrology and*  
1426 *Earth System Sciences*, *25*(6), 3397-3409.
- 1427 Siemers, J., & Dreybrodt, W. (1998). Early development of Karst aquifers on percolation  
1428 networks of fractures in limestone. *Water Resour. Res.*, *34*, 409–419.  
1429 <https://doi.org/10.1029/97WR03218>
- 1430 Simms, M.J. (2004). Tortoises and hares: dissolution, erosion and isostasy in landscape  
1431 evolution. *Earth Surf. Process. Landforms*, *29*, 477–494. <https://doi.org/10.1002/esp.1047>
- 1432 Smith, D.I., & Atkinson, T.C. (1976). Process, Landforms and Climate in Limestone Regions.  
1433 *Geomorphology and climate*, *512*.
- 1434 Spellman, P., Gulley, J., Martin, J. B., & Loucks, J. (2019). The role of antecedent groundwater  
1435 heads in controlling transient aquifer storage and flood peak attenuation in karst watersheds.  
1436 *Earth Surface Processes and Landforms*, *44*(1), 77-87.
- 1437 Spötl, C., Fairchild, I. J., & Tooth, A. F. (2005). Cave air control on dripwater geochemistry,  
1438 Obir Caves (Austria): Implications for speleothem deposition in dynamically ventilated caves.  
1439 *Geochimica et Cosmochimica Acta*, *69*(10), 2451-2468.  
1440 <https://doi.org/10.1016/j.gca.2004.12.009>
- 1441 Stock, G.M., Granger, D.E., Sasowsky, I.D., Anderson, R.S., & Finkel, R.C. (2005). Comparison  
1442 of U–Th, paleomagnetism, and cosmogenic burial methods for dating caves: implications for  
1443 landscape evolution studies. *Earth and Planetary Science Letters*, *236*(1-2), 388-403.

- 1444 Ström, L., Owen, A. G., Godbold, D. L., & Jones, D. L. (2005). Organic acid behaviour in a  
1445 calcareous soil implications for rhizosphere nutrient cycling. *Soil Biology & Biochemistry*, *37*,  
1446 2046–2054.
- 1447 Sullivan, P.L., Stops, M.W., Macpherson, G.L., Li, L., Hirmas, D.R., & Dodds, W.K. (2019).  
1448 How landscape heterogeneity governs stream water concentration-discharge behavior in  
1449 carbonate terrains (Konza Prairie, USA). *Chemical Geology*, *527*, 118989.  
1450 <https://doi.org/10.1016/j.chemgeo.2018.12.002>
- 1451 Sullivan, P.L., Wymore, A.S., McDowell, M., Aarons, S., Aciego, S., Anders, A.M., et al.  
1452 (2017). New opportunities for Critical Zone science, In: *2017 CZO Arlington Meeting White*  
1453 *Booklet*.
- 1454 Sullivan, P. L., Zhang, C., Behm, M., Zhang, F., & Macpherson, G. L. (2020). Toward a new  
1455 conceptual model for groundwater flow in merokarst systems: Insights from multiple  
1456 geophysical approaches. *Hydrological Processes*, *34*(24), 4697–4711.
- 1457 Svensson, U., & Dreybrodt, W. (1992). Dissolution kinetics of natural calcite minerals in CO<sub>2</sub>-  
1458 water systems approaching calcite equilibrium. *Chemical Geology*, *100*, 129–145.
- 1459 Swaffer, B. A., Holland, K. L., Doody, T. M., Li, C., & Hutson, J. (2014). Water use strategies of  
1460 two co-occurring tree species in a semi-arid karst environment. *Hydrological Processes*, *28*,  
1461 2003–2017.
- 1462 Szymczak, P., & Ladd, A.J.C. (2011). The initial stages of cave formation: Beyond the one-  
1463 dimensional paradigm. *Earth and Planetary Science Letters*, *301*, 424–432.
- 1464 Szymczak, P., & Ladd, A.J.C. (2012). Reactive-infiltration instabilities in rocks. Fracture  
1465 dissolution. *J. Fluid Mech.*, *702*, 239–264. <https://doi.org/10.1017/jfm.2012.174>  
1466 <https://doi.org/10.1016/j.epsl.2010.10.026>

- 1467 Tennyson, R., Brahana, V., Polyak, V.J., Potra, A., Covington, M., Asmerom, Y., et al. (2017).  
1468 Hypogene Speleogenesis in the Southern Ozark Uplands, Mid-Continental United States, In:  
1469 Klimchouk, A. N., Palmer, A., De Waele, J., S. Auler, A., & Audra, P. (Eds.), *Hypogene Karst*  
1470 *Regions and Caves of the World*. Springer International Publishing, Cham, pp. 663–676.  
1471 [https://doi.org/10.1007/978-3-319-53348-3\\_43](https://doi.org/10.1007/978-3-319-53348-3_43)
- 1472 Tooth, A.F., & Fairchild, I.J. (2003). Soil and karst aquifer hydrological controls on the  
1473 geochemical evolution of speleothem-forming drip waters, Crag Cave, southwest Ireland.  
1474 *Journal of Hydrology*, 273, 51–68. [https://doi.org/10.1016/S0022-1694\(02\)00349-9](https://doi.org/10.1016/S0022-1694(02)00349-9)
- 1475 Torres, M. A., A. J. West, & Li, G. (2014). Sulphide oxidation and carbonate dissolution as a  
1476 source of CO<sub>2</sub> over geological timescales, *Nature*, 507(7492), 346-349.
- 1477 Troester, J. W., White, E. L., & White, W. B. (1984). A comparison of sinkhole depth frequency  
1478 distributions in temperate and tropic karst regions. In *Multidisciplinary conference on sinkholes*.  
1479 *I* (pp. 65-73).
- 1480 Vacher, H.L., & Mylroie, J.E. (2002). Eogenetic karst from the perspective of an equivalent  
1481 porous medium. *Carbonates and Evaporites*, 17, 182.
- 1482 Vesper, D. J., & White, W. B. (2004). Storm pulse chemographs of saturation index and carbon  
1483 dioxide pressure: implications for shifting recharge sources during storm events in the karst  
1484 aquifer at Fort Campbell, Kentucky/Tennessee, USA. *Hydrogeology Journal*, 12(2), 135-143.  
1485 <https://doi.org/10.1007/s10040-003-0299-8>
- 1486 Wagner, T., Fritz, H., Stüwe, K., Nestroy, O., Rodnight, H., Hellstrom, J., et al. 2(011).  
1487 Correlations of cave levels, stream terraces and planation surfaces along the River Mur—Timing  
1488 of landscape evolution along the eastern margin of the Alps. *Geomorphology*, 134, 62–78.  
1489 <https://doi.org/10.1016/j.geomorph.2011.04.024>

- 1490 Wen, H., Sullivan, P. L., Macpherson, G. L., Billings, S. A., & Li, L. (2021). Deepening roots  
1491 can enhance carbonate weathering by amplifying CO<sub>2</sub>-rich recharge. *Biogeosciences*, *18*(1), 55-  
1492 75.
- 1493 White, W.B. (2002). Karst hydrology: recent developments and open questions. *Engineering*  
1494 *Geology*, *65*, 85–105. [https://doi.org/10.1016/S0013-7952\(01\)00116-8](https://doi.org/10.1016/S0013-7952(01)00116-8)
- 1495 White, W.B. (1984). Rate processes: chemical kinetics and karst landform development. In  
1496 *Groundwater as a Geomorphic Agent*. Routledge: London.  
1497 <https://doi.org/10.4324/9781003028833>
- 1498 White, W.B., Herman, E., Rutigliano, M., Herman, J., Vesper, D., & Engel, S. (2016). Karst  
1499 groundwater contamination and public health. *Karst Waters Inst. Spec. Publ. 19*, Springer.
- 1500 White, W.B., & White, E.L. (2005). Size scales for closed depression landforms: The place of  
1501 tiankengs. *Cave and Karst Science*, *32*(2/3), 111.
- 1502 Wigley, T.M.L., & Plummer, L.N. (1976). Mixing of carbonate waters. *Geochimica et*  
1503 *Cosmochimica Acta*, *40*, 989–995. [https://doi.org/10.1016/0016-7037\(76\)90041-7](https://doi.org/10.1016/0016-7037(76)90041-7)
- 1504 Williams, P. (2008a). The role of the epikarst in karst and cave hydrogeology: a review.  
1505 *International Journal of Speleology*, *37*. <http://dx.doi.org/10.5038/1827-806X.37.1.1>
- 1506 Williams, P. (2008b). *World Heritage Caves and Karst: A thematic study*. Gland, Switzerland:  
1507 IUCN 57pp.
- 1508 Williams, P.W. (1985). Subcutaneous hydrology and the development of doline and cockpit  
1509 karst. *Zeitschrift für Geomorphologie*, *29*, 463–482.
- 1510 Wolfe, B. T., & Kursar, T. A. (2015). Diverse patterns of stored water use among saplings in  
1511 seasonally dry tropical forests. *Oecologia*, *179*, 925–936.
- 1512 Wong, C.I., Banner, J.L., & Musgrove, M. (2011). Seasonal dripwater Mg/Ca and Sr/Ca  
1513 variations driven by cave ventilation: Implications for and modeling of speleothem paleoclimate

- 1514 records. *Geochimica et Cosmochimica Acta*, 75, 3514–3529.  
1515 <https://doi.org/10.1016/j.gca.2011.03.025>
- 1516 Wood, W.W. (1985). Origin of caves and other solution openings in the unsaturated (vadose)  
1517 zone of carbonate rocks: A model for CO<sub>2</sub> generation. *Geology*, 13, 822–824.
- 1518 Wood, W.W., & Petraitis, M.J. (1984). Origin and Distribution of Carbon Dioxide in the  
1519 Unsaturated Zone of the Southern High Plains of Texas. *Water Resour. Res.*, 20, 1193–1208.  
1520 <https://doi.org/10.1029/WR020i009p01193>
- 1521 Worthington, S.R. (1999). A comprehensive strategy for understanding flow in carbonate  
1522 aquifers, in: *Karst Modeling, Karst Waters Institute Special Publication 5. Karst Waters*  
1523 *Institute*, pp. 30–37.
- 1524 Worthington, S.R.H. (2009). Diagnostic hydrogeologic characteristics of a karst aquifer  
1525 (Kentucky, USA). *Hydrogeol J*, 17, 1665–1678. <https://doi.org/10.1007/s10040-009-0489-0>
- 1526 Worthington, S.R.H., Davies, G.J., & Alexander, E.C. (2016). Enhancement of bedrock  
1527 permeability by weathering. *Earth-Science Reviews*, 160, 188–202.  
1528 <https://doi.org/10.1016/j.earscirev.2016.07.002>
- 1529 Wray, R.A.L., & Sauro, F. (2017). An updated global review of solutional weathering processes  
1530 and forms in quartz sandstones and quartzites. *Earth-Science Reviews*, 171, 520–557.  
1531 <https://doi.org/10.1016/j.earscirev.2017.06.008>
- 1532 Zeng, Q., Liu, Z., Chen, B., Hu, Y., Zeng, S., Zeng, C., et al. (2017). Carbonate weathering-  
1533 related carbon sink fluxes under different land uses: A case study from the Shawan Simulation  
1534 Test Site, Puding, Southwest China. *Chemical Geology*, 474, 58–71.
- 1535 Zhao, L., & Hou, R. (2019). Human causes of soil loss in rural karst environments: a case study  
1536 of Guizhou, China. *Scientific Reports*, 9(1), 1-11. doi:10.1038/s41598-018-35808-3

- 1537 Zorn, M., Erhartic, B., Komac, B., & Gauchon, C. (2009). La Slovénie, berceau du géotourisme  
1538 karstique. *Karstologia*, 54(1), 1–10. <https://doi.org/10.3406/karst.2009.2655>